INFLUENCE OF DEFECTS ON THERMAL AND MECHANICAL PROPERTIES OF METALS

A Thesis

by

SANDEEP KUMAR KAMANI

Submitted to the Office of Graduate Studies of
Texas A&M University
in partial fulfillment of the requirements for the degree of

MASTER OF SCIENCE

August 2008

Major Subject: Chemical Engineering

INFLUENCE OF DEFECTS ON THERMAL AND MECHANICAL PROPERTIES OF METALS

A Thesis

by

SANDEEP KUMAR KAMANI

Submitted to the Office of Graduate Studies of
Texas A&M University
in partial fulfillment of the requirements for the degree of

MASTER OF SCIENCE

Approved by:

Chair of Committee,	Tahir Cagin
Committee Members,	Sam Mannan
	Xinghang Zhang
Head of Department,	Michael Pishko

August 2008

Major Subject: Chemical Engineering

ABSTRACT

Influence of Defects on Thermal and Mechanical Properties of Metals. (August 2008)

Sandeep Kumar Kamani, B. Tech., Andhra University

Chair of Advisory Committee: Dr. Tahir Cagin

The crystallization/freezing and melting phenomena are critical in processing of chemicals and materials. Although melting is a very fundamental problem, the mechanism behind it has not been completely answered satisfactorily. Hence its study becomes very important. Perfect crystals do not exist; therefore it is very important to include the effect of defects in the above mentioned processes. The purpose of this work is to employ molecular simulation to further extend the understanding of theories of melting with respect to defects. We studied the melting and freezing process for a model system of copper with and without defects. We studied point defects (1, 2, 4, 8 vacancies and 1, 2, 4, 8 interstitials), line defects (edge dislocation) and surface defects (grain boundary) using molecular dynamics simulations. Constant stress-constant temperature ensemble with atmospheric pressures is employed. Various properties like average volume, density, potential energy and total energy are obtained as a function of temperature for each system. Most of the properties vary linearly before and after the phase transitions. During the transition process they show a dramatic change. This change is a sign of phase transition. The phase transition temperatures obtained from the single phase simulations are not the true melting (or freezing) points as there is some

amount of superheating (or supercooling). Coexistence phase simulations are also done for the case of copper with no defects to find the true melting point. Most of the literature dealing with melting/crystallization on the basis of atomistic simulation does not include the influence of the presence of defects. Thus this work has a bearing on the various theories of melting.

To my parents and brothers

ACKNOWLEDGEMENTS

I take this opportunity to express my sincere appreciation to Dr. Tahir Cagin for his advice, guidance and assistance over the last two years. He has been always available to help me move ahead in the project whenever there was a hurdle. He has been very patient when I could not get something done and has always motivated me to try out new ideas. His kind help has made this thesis possible. I extend my gratitude to the members of my advisory committee, Dr. Sam Mannan and Dr. Xinghang Zhang, for their time.

I would also like to express my appreciation to all my colleagues especially Arnab Chakrabarty, Oscar Ojeda, Bedri Arman, Roy Araujo, Hieu Pham, Justin Haskins, Jennifer Carvajal, Alper Kinaci and others for their support, patience, friendship and for making my stay at Texas A&M a very pleasant experience. I would like to thank Jeff Polasek for helping me out with the software needs during this time. Last, and definitely not the least, I thank my family for their constant love, encouragement and support. My parents' faith and sacrifices over the years have always kept me moving forward towards my goals.

TABLE OF CONTENTS

Page

ABSTRACT iii

DEDICATION v

ACKNOWLEDGEMENTS vi

TABLE OF CONTENTS vii

LIST OF TABLES ix

LIST OF FIGURES x

LIST OF SYMBOLS xiii

CHAPTER

I INTRODUCTION 1

Vacancy clustering 6

II BACKGROUND 9

Crystalline solids 9
Types of defects 12
Point defects 12
Dislocations 14
Grain boundaries 15
Molecular simulations 15

III PROCEDURE 21

Structures 21
Vacancy and interstitial 21
Edge dislocation 23
Grain boundary 24
Phase-coexistence simulation 27
Solid 27
Liquid 28
Quantum Sutton Chen potential 31
Single phase simulations 32

CHAPTER Page

Phase-coexistence simulations 36

IV RESULTS AND DISCUSSION 38

Single phase simulations 38
Vacancies and interstitials 47
Edge dislocation 52
Grain boundary 1 54
Grain boundary 2 58
Phase-coexistence simulations 61
Vacancy clustering 69

V CONCLUSION 71

REFERENCES 74

VITA 84

LIST OF TABLES

TABLE Page

1 Parameters for the SC and QSC many-body potential for Cu..... 32

2 Linear expansion of copper as a function of temperature 38

3 Melting and freezing points of copper with various number of defects.. 49

4 Vacancy formation energies for a single vacancy for copper 69

5 Binding energies of divacancies in eV 70

LIST OF FIGURES

FIGURE		Page
1	An example of point defects in a crystal; (a) vacancy ; (b) interstitial ...	13
2	2X2X2 supercell of copper with a vacancy.....	19
3	2X2X2 supercell of copper with an interstitial	19
4	CERIUS^{2TM} developed by Accelerys.....	20
5	Copper with 8 interstitials (different colored atoms) initial structure.....	22
6	Copper edge dislocation	23
7	GB STUDIO interface.....	24
8	Grain boundary structure 1 : sigma 3, <111>, 60^0	25
9	Grain boundary structure 2: Sigma 5, <210>, 180^0.....	26
10	Copper liquid-solid interface for two-phase simulation.....	30
11	Supercell of 864 atoms of Cu.....	33
12	Unit cell of Cu (FCC) created using XCrySDen.....	33
13	Copper with 8 interstitials at 1600K	34
14	Temperature Vs time for copper without defects at 1360K	39
15	Potential energy Vs time for copper without defects at 1360K	40
16	Total energy Vs time for copper without defects at 1360K	40
17	Average volume Vs temperature for pure copper without defects.....	41
18	Total energy Vs temperature for copper without defects	41
19	Density Vs temperature for copper without defects.....	42
20	Potential energy Vs temperature for copper without defects	42

FIGURE Page

21 Radial distribution function at 600K, 1355K and 1600K for Cu without defects 43

22 Kinetic energy Vs temperature for copper without defects..... 45

23 Heat capacity Vs temperature for copper without defects 45

24 Freezing points Vs number of defects..... 46

25 Melting point Vs number of defects..... 46

26 Fractional increase in lattice parameter Vs concentration of point defects at 300K..... 47

27 Average volume per atom Vs temperature for Cu with 0, 1, 2, 4 and 8 vacancies..... 48

28 Average volume per atom Vs temperature for Cu with 0, 1, 2, 4 and 8 interstitials 48

29 Melting point Vs number of vacancies 50

30 Melting point Vs number of interstitials 51

31 Edge dislocation at 600K 52

32 Edge dislocation at 600K 53

33 A unit cell of grain boundary structure using GBStudio..... 54

34 Density Vs temperature for grain boundary structure 1 56

35 Average volume Vs temperature for grain boundary structure 1..... 56

36 Density Vs temperature for copper (6X6X8 lattice) without defects..... 57

37 Average volume Vs temperature for copper (6X6X8 lattice) without defects 57

38 Radial distribution function at 1000K, 1350K and 1370K for grain boundary 1 58

FIGURE Page

39 Density Vs temperature for copper grain boundary 2 59

40 Average volume Vs temperature for copper grain boundary 2 59

41 Radial distribution function at 1000K, 1270K and 1400K for grain boundary 2 60

42 Phase coexistence simulation of copper at 900K at 0 ps (starting structure) 62

43 Phase coexistence simulation of copper at 900K at 20 ps 62

44 Phase coexistence simulation of copper at 950K after 10ps 63

45 Phase coexistence simulation of copper at 950K after 30ps 63

46 Phase coexistence simulation of copper at 1000K after 20ps 64

47 Phase coexistence simulation of copper at 1100K after 10ps 64

48 Phase coexistence simulation of copper at 1050K at 0ps (starting structure) 65

49 Phase coexistence simulation of copper at 1050K after 5ps 65

50 Phase coexistence simulation of copper at 1050K after 15ps 66

51 Phase coexistence simulation of copper at 1050K after 25ps 66

52 Radial distribution function of coexistence phase simulations at 900K, 1000K and 1100K 67

LIST OF SYMBOLS

T	absolute temperature
P	pressure
V	volume
N	number of atoms
E	energy
T_m	melting temperature
T_f	freezing point
a_0	lattice constant
x, y, z	the three Cartesian coordinates
α, β, γ	Cartesian indices
ΔS	change in entropy
m	mass
H	Enthalpy
U, PE	potential function
KE	kinetic energy
TE	total energy
α_t	thermal expansion coefficient
η	order parameter
S(k)	structure factor
Fcc	face-centered cubic
Bcc	body-centered cubic

Hcp	hexagonal close packed
MD	Molecular Dynamics
MC	Monte-Carlo
3D	three-dimensional
C_{44}	< 100 > shear modulus
C’	< 110 > shear modulus
1NN	first nearest neighbor
2NN	second nearest neighbor
APF	atomic packing factor
N_v	number of point defects
H_f	defect formation energy
GB	Grain boundary
a_{1200}	lattice parameter at 1200K
V_{1200}	volume at 1200K
$V(r_{ij})$	pair wise potential
r_{ij}	the distance between atoms *i* and *j*
SC	Sutton Chen
QSC	Quantum Sutton Chen
C_p	Heat capacity
ps	picosecond
RDF	Radial distribution function
TtN	constant stress-constant temperature ensemble

CHAPTER I

INTRODUCTION

The melting and crystallization/freezing phenomena are critical in processing of chemicals and materials. Some of the applications include metal forming, sintering, casting, protein crystallization and processing of pharmaceuticals. Melting is one of the most common phenomena known, yet it's the most difficult to understand. Melting is a process in which a crystal undergoes a phase change from a solid to a liquid. Understanding the mechanism behind this process is still a challenge. The theory of melting has been an issue which has stayed with the science community since a long time. Although there have been quite a few theories proposed by many scientists, there still remains a large number of questions that are still unanswered. These theories mainly consider homogeneous melting process.

Some laws like the one proposed by Lindemann, although very simple does not take many factors into consideration; it forms a basis which helps explain some fundamental mechanisms. Lindemann suggested that melting occurs when the amplitude of atomic thermal vibrations exceed a fraction of the inter-atomic spacing. One of the main drawbacks of this law is that he does not take into account the fact that melting actually involves bond breaking. Lindemann's law has been studied for different materials[1,2] and model fluids[3,4]. A lot of investigation has been done on Lindemann's law[1,5-18].

This thesis follows the style and format of the *Journal of Physical Chemistry B.*

Born[19] suggested that melting occurs as a result of the vanishing of shear elastic coefficient. He observed that, unlike the crystal phase, the liquid phase does not offer any resistance to shear stress. Kanigel et al[20] through their molecular dynamics simulation have also obtained that at melting the Born criterion is satisfied and show that one of the shear moduli of the solid vanishes. Granato proposed a model that consisted of interstitials coupled to shear strains[21].

The Hansen-Verlet freezing rule [7] states that the amplitude S_m of the first maximum in the structure factor S(k) has to be more than 2.85 for a liquid of three dimensional to freeze and it goes up to around 5.5 [22] when two dimensional freezing is considered. Another criterion for crystallization of Brownian colloidal fluids was proposed by L¨owen, Palberg and Simon (LPS) [3].

Frenkel proposed that melting occurs due to the generation and spreading of intrinsic crystalline defects like vacancies[23]. Lenard-Jones and Devonshire[24,25] proposed a theory based on positional disordering. They considered a model of rare-gas crystal and the first order phase transition was observed. Their theory was based on a "order-disorder" transition. The inadequacy in this theory was that it proposed a critical point for melting which was not observed experimentally[24,25]. The dislocation theory of melting is also studied and supported by Cotterill[26].

According to Jin *et al.*[16], both the Lindemann and Born criteria are behind the mechanism of melting. They say that the superheating limit is decided by the vibrational and elastic instability criteria as well as the homogeneous nucleation theory.

According to Górecki[27,28], vacancy concentration suddenly increases from a value of ~0.37% to 10% on melting. This increase in vacancy concentration on melting is said to have been due to the melting of the surface[29].

Superheating has been observed even in surface systems[30-32]. Superheating is hardly observed for fcc(110) and fcc(100) surfaces[33-35]. Surface can be omitted either by coating the system with another system with higher melting point[36], or internal heating[37] or computationally it can be done by applying three dimensional periodic boundary conditions to a finite sized system. Unlike superheating, supercooling is more common phenomena. Earlier studies have shown that the grain boundaries cannot melt below the true melting temperature[38-47].

Modeling can be done either by first principle calculations, which are more accurate, or by using Molecular Dynamics[48]. The former cannot be used for large systems. For the present calculations such rigorous method is not required. The aim is to do a qualitative study and not a quantitative one. Hence Molecular Dynamics is chosen which takes into consideration atomic interactions. A larger system of around 1000 atoms is chosen.

Experimentally it is difficult to measure melting process inside a crystal as the whole process occurs in a small interval of time. It is here that MD Simulation techniques play a vital role in determining various structures and properties. Experimentally it is difficult to exclude various types of imperfections like point defects, dislocations, surfaces and grain boundaries in every case but through MD one can obtain perfect crystal structures. The Molecular Dynamic simulations provide all the

information of atomic movements and behavior at a comparable time scale. It is important to study the atomic level interactions of the fcc transition metals to develop their technological applications. Among the closed packed structures copper is chosen for the study. This is due to the fact that it is a good system to study and there is sufficient experimental data available. But the focus of this work is not on copper by itself, the aim is to study metals in general. Melting studies has been done by various researchers looking at different aspects. This work looks at it from a point of view of defects and how the melting point and other properties would vary with respect to point defects like vacancies and interstitials; dislocations, and even grain boundaries

In this work the focus is on the influence of defects including vacancies and interstitials, on the mechanical and thermal properties of Metals, using copper as an example. Here the variation of the melting point of copper with the number of defects is studied. Some groups have done studies on clusters of various sizes. What is expected is that when there is a vacancy for example, it is like a pre-existent gap and so on heating it gets easier for it to enlarge and hence melt faster. Thus it is expected that melting point decreases as number of vacancy increases. When there is an interstitial, there are more atoms and they are crowded. The presence of an extra atom might cause distortion of the lattice which might help in melting.

When three dimensional (3D) periodic boundary conditions are used in MD simulations of a bulk crystal, temperature hysteresis is obtained[49-53]. This is because it does not take surface effects into consideration and it resembles a bulk structure. The melting occurs at a higher temperature. In experiments, the melting that occurs is due to

heterogeneous nucleation where due to the presence of defects, nucleation sites are provided which help in phase transition. In the past simulations for copper atoms of different sizes have been done using Monte Carlo Simulations [54] and also by Molecular Dynamic Simulations[55]. Thermodynamic properties of copper have been studied using Molecular Dynamics by Mei and coworkers[56].

The hysteresis effect is avoided to obtain the true melting point of the crystal. One method that is used is by calculating the free energy of a system which would be equal for both phases at the transition temperature. Calculation of free energy is first of all not easy and it should be highly accurate so as to get the correct temperature. The other method to calculate the true melting point of a crystal is by performing two-phase simulations.

Wu Zhi-Min and coworkers studied the melting and freezing processes for copper with various numbers of atoms using the microcanonical molecular dynamics simulation technique and found that they increase almost linearly with increasing atom numbers in the cluster. They also reported hysteresis effect in copper nanoclusters[55]. It has also been shown that small clusters melt before the bulk metal[57,58]. Another group studied the melting and structural transition of small copper clusters and found that the melting temperature is proportional to the average coordination number[59].

Luo et al. earlier studied the disordering of defective stishovite at high temperature and zero pressure using molecular dynamics simulations. According to them various defects initiate or facilitate solid-state disordering and melting [60].

Dederichs et al found a reduction in the values of C_{44} and C' along with a small concentration of vacancies at 0K[61]. But they used a two body potential which is not very reliable. Kanigel et al[20] found C_{44} to be independent of concentration of vacancies at any temperature until the melting point. Interstitials, in general were found to have caused anisotropic softening of shear moduli[20,61,62]. Unlike this work, Kanigel et al[20] found that vacancies have no effect on melting. Concentration of vacancies as large as 4% did not have any effect on melting point in their case. The reason that they provided for this was that atomic volume is larger than specific volume per vacancy. They found that interstitials decrease the melting point [20].

Vacancy clustering

Point defects and especially vacancies play a very important role in various phenomena metals. Hence, study of vacancies and their interactions in metals is critical in understanding kinetic and thermodynamic properties of metals.

Irradiation generates vacancies which come together to form divacancies, divacancies diffuse to form a cluster of vacancies [63] which in turn form a prismatic dislocation loop [64-69]. This is a problem especially in nuclear reactors because the radiation eventually makes the metal brittle. Thus study of various vacancies, their interaction and their properties at high temperatures becomes valuable.

The above mentioned mechanism is supported by MD calculations done for iron [70]. But Carling et al. [71] did first principle calculations for Al and found out that the nearest neighbor divacancy formation energy is negative and hence not coherent with the

experiments which say that divacancies are stable [72,73]. They found first nearest neighbor (1NN) and second nearest neighbor (2NN) binding energies as -0.08eV and +0.004ev respectively. Uesugi et al. [74] got similar value for 1NN binding energy and their value for 2NN was +0.04. According to them the 2NN divacancy in Al is stable as it is in the same range of the 1NN divacancy binding energy of Cu[75]. This trend was obtained for Al and might not be the case with other metals. For Mg both 1NN and 2NN divacancies were found to be stable with positive binding energies [74]. The concentration of vacancies is very low in metals [72]. Thus quantum mechanical calculations which are performed on a system with very high concentration of vacancies might not give realistic results.

Gavini et al. [76] used quasi-quantum orbital-free density-functional theory (QCOFDFT) [77] for very low defect concentration in aluminum which they obtained by using millions of atoms, to find the concentration dependence of binding energy of divacancies [76]. Through their calculations they have demonstrated that the vacancies are attractive for very low and realistic concentration in accordance with experiment [73,78], whereas for higher concentrations the same vacancies are repulsive. They also found that divacancies attract to form quadvacancies as they have positive binding energies. Quadvacancies concentration dependence was found to follow same trend as that of the divacancies. They have also observed a formation of high stable configuration of prismatic dislocation loop from a hexagonal cluster having seven vacancies on (111) plane. This structure was found to be more stable than the other uncollapsed stable configuration. But multiple vacancies when placed on (110) plane did not yield similar results.[64]

Carling et al. [71] have also used MD to study the normalized temperature dependence of Al for the monovacancy formation energy. This has also been observed for Cu [79]. It is difficult to study vacancies either experimentally or theoretically due to very small concentration that is required to get realistic results. Vacancies have been studied for simple metals [80-90] and transition metals [91-96]. There is also experimental data for vacancy formation energies[78,97,98]. Korhenen et al. [95]have calculated vacancy-formation energies for fcc and bcc transition metals using first-principles. Their results seem to be close to experimental data for fcc metals but not for bcc metals. The energy of formation of a vacancy is an important aspect in defect studies. Experimental divacancy binding energy is reported by Balluffi et al.[99].

CHAPTER II

BACKGROUND

Crystalline solids

Unlike amorphous state, which is disordered, crystals are solids which have an atomic structure which is formed by repetition of a smaller structure many number of times. Hence they are periodic and highly symmetric structures. These are known as perfect crystals. The smallest structure which is repeated to form the larger structure is called a unit cell. Positions of rest of the atoms of the crystal can be found by translating the unit cell parallel to the edges in all three directions. Each point where there is an atom is called a lattice point. All lattice points are identical. The directions along which the unit cell is repeated are called a basis vectors. The length of the unit cell in each direction is called the lattice parameter or lattice constant. The angle between these is also an important characteristic. The lattice parameter may or may not be equal depending on the property of the crystal. Thus crystalline materials are those with repetitive structures. Liquid structure on the other hand has no pattern as can be seen in the figure on page 34. Generally the orthogonal coordinate system is convenient to study the crystal structure. There are 14 types of Bravis lattices, which are mainly different possible crystal structures depending on the lattice constants. Out of these we only consider the most important ones which are the close-packed structures. Atoms usually tend to pack as close as possible making the density higher. There are three important

crystal structures: Face-centered cubic (FCC), Body-centered cubic (BCC) and Hexagonal close-packed (HCP)

a) Face-centered cubic crystal structure (FCC): In this kind of structure, atoms are located at eight corners of a unit cell and 6 face centers of a cube. Metals like copper, gold, silver, aluminum, lead, platinum etc have this kind of structure. There are 4 atoms per unit cell in fcc. The coordination number for fcc is 12 and atomic packing factor 0.74.

b) Body-centered cubic crystal structure (BCC): In this kind of structure, atoms are located at eight corners of a unit cell and one at the body center of a cube. Metals like chromium, iron, molybdenum, tantalum, tungsten etc have this kind of structure. There are 2 atoms per unit cell in bcc. The coordination number for bcc is 8 and atomic packing factor is 0.68.

c) Hexagonal closed-packed crystal structure (HCP): In HCP, the unit cell is hexagonal rather than cubic. In this structure, there are six atoms forming a hexagon on each of the two faces parallel to each other. These six atoms also have another atom at the center. Between these two planed, there is another plane that has three more atoms. Totally there are 6 atoms per unit cell in hcp. The coordination number for hcp is 12 and atomic packing factor is 0.74. Since it is not cubic, there exist a short (a) and a long (c) length of the unit cell, with the ideal c/a ratio being 1.633 which can be calculated for the geometry.

One more aspect which is important is point groups, which are point symmetry operations. In these operations the origin is fixed and other points are rotated by a certain degrees. Crystalline materials usually involve metallic or ionic bonding (non-directional). Most metals and alloys, many ceramics and some polymers are of this type. Face-centered cubic (FCC): Example Cu, Ni, Al, Ag, Au, Pb, Pt etc. There are 4 atoms in a unit cell. The coordination number for fcc unit cell is 12. Atomic packing factor for fcc crystal is 0.74.

APF = (Volume of atoms in unit cell) / (Volume of unit cell)

As the materials scientist F. C. Franck once said,

"Crystals are like people; it is only the defects that make them interesting".

There is nothing such as perfect crystals where every atom is in its correct position. In reality, crystals generally have imperfection, or what are known as crystal defects. These may be point defects like vacancies and interstitials, although their concentration is usually considered to be low. Other types of defects like dislocations and grain boundaries might also be present. There might also be impurities present in the crystals. Sometimes even marginal amount of impurities can give rise to various properties in materials. Example, a small amount of impurity might be the reason for the conductivity of some semiconductors.

Types of defects

The crystal defects can be categorized into the following[100]:

a) Point defects (0 dimension): Vacancies, Interstitials, impurities
b) Line defects (1 dimension): Dislocations
c) Planar defects (2 dimensions): external surfaces, grain boundary, twin boundary, stacking faults, phase boundaries
d) Volume defects(3 dimensions): precipitates, inclusion, pores/voids, cracks, other phases

Point defects: Point defects are intrinsic in nature. They affect the chemical properties of the solid. Controlled point defects have wide range of applications like transistors, integrated circuits, photo sensors, color-television, fluorescent lamps etc. [101]

- Vacancy: This is one of the simplest forms of imperfection. When an atom leaves its position, there is a vacant position created which is known as a Vacancy. Presence of a vacancy will increase randomness and hence entropy.
- Self-interstitial: In this type of defect, there is an extra atom that is present in the space between the atoms of the crystal lattice. Due to the presence of an extra atom there is distortion of the crystal lattice structure which also brings about disorder. The interstitial atoms might be of the same element type or it also might be an impurity. This impurity can have a huge effect on the properties of the crystal.

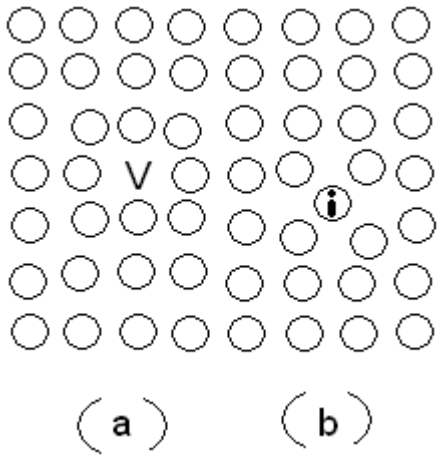

Figure 1: An example of point defects in a crystal; (a) vacancy; (b) interstitial

In figure 1, V is a vacant site where there was supposed to be an atom had it been a perfect crystals. The atom which is labeled 'i' is an interstitial atom which is at a non-lattice site.

In homogeneous materials, point defects are generally produced by high-energy particle irradiation, plastic deformation or under conditions of thermal equilibrium. The equilibrium concentration of defects is given by the relation:

$$c = \frac{N_v}{N} = e^{-\frac{H_V}{kT}}$$

c = concentration of point defect

N_v = Number of point defects

N = Total number of atoms

H_f = defect formation energy (eV/atom)

k_B = Boltzmann constant = $1.37 * 10^{-23}$ (Watt*sec*degree^{-1})

T = absolute temperature (K)

This is at the situation of minimum free energy. If *ln c* is plotted as a function of *(1/T)*, a straight line is obtained, the slope of which is known if we know H_f. The energy of formation of a defect is an important aspect in defect studies as it helps understand the thermal behavior of materials. In case of vacancy, H^v_f is the energy required to remove an atom from its lattice position to the surface of the crystal and in case of interstitial, H^i_f is the energy associated to move an atom from the surface and place it between the atoms. Usually the formation energy of interstitials is a couple of times higher than that of a vacancy. If n point defects are introduced in the lattice, the change in free energy would be[102]

$$\Delta F = nH_f - T\Delta S$$

H_f is the energy of formation of a defect

ΔS is the change in entropy of crystal

There is an approximate rule which says that $H_f \approx 8kT_m$. [102]

Formation energy[100] of vacancy of copper = 0.8 – 1 eV

Point defects usually are free to move, and they do so by exchanging place with neighboring atom.

Dislocations: Dislocation or the so called line defects are formed when a row of atoms is missing from its lattice position. This missing row causes a distortion in the arrangement of the atoms around it. This may also be considered as a slipping of a layer of atoms from its equilibrium position. This has an effect on the rows of atoms beside this missing row since there is a difference in the density of atoms in a direction

perpendicular to the line defect. Unlike point defects, like defect does not have any effect on the electronic properties. [101]

Grain boundaries: When crystalline solids orient differently in different parts of crystals, each orientation is called a grain and the boundary between two such grains is called a grain boundary. Every grain is like a single crystal but with different orientation. The importance of grain boundary in polycrystalline materials is realized in the processes like high temperature creep, superplasiticity, recrystallization, yielding and embrittlement[100].

Molecular simulations

This part will talk about the various methods of simulation that exist and methods that are used here for calculations. A general understanding of Molecular Dynamics is also given. Modeling and Simulation is very important part of theory and experiment and is applicable to a wide variety of problems in various fields. With Molecular Dynamics modeling the position of every atom is traced as it moves from its lattice position. It is a very useful tool in studying the phase transition. When performing a Molecular Simulation, first an input structure is needed, which is called the system. This system has a certain number of atoms arranged in a particular manner. Now these atoms interact among themselves. Hence there is also a need to define how these atoms interact with one another. This is one of the most important input parameter and is defined by what is known as a “force field” or an inter-atomic potential. There are a large number of

force fields that are present and one of them is chosen to suit the type of system that we consider based on previous study and also on our requirements. Depending on how close the results are with experiments, the accuracy of the force field is defined. It is the force fields that determine the complexity of Molecular Dynamic simulations. Now the initial position at $t = t_0$ is known and the way the atoms interact is known, so how and where the atom is going to move after a small time at $t = t_0 + \Delta t$ can be calculated. Here Δt is called the timestep and this should be kept small so that calculations are accurate. Hence the trajectory of the atoms along with time can be tracked in a similar manner by increasing the time. This type of detailed information is not easy to obtain using experiments. So studying the movement of all the atoms together provides an understanding of the material behavior, say phase change in the present case.

$$F^t = ma^t$$

$$v_i(t) = \frac{dr_i(t)}{dt}$$

$$a_i(t) = \frac{dv_i(t)}{dt} = \frac{d^2(r_i)}{dt^2}$$

$$r_i(t) = r_i(t_0 + \Delta t) = r_i(t_0) + v_i(t_0)\Delta t + \frac{1}{2}a_i(t_0)(\Delta t)^2 + ...$$

$$v_i(t) = v_i(t_0 + \Delta t) = v_i(t_0) + a_i(t_0)\Delta t$$

$$t = t_0 + \Delta t$$

$$KE = \frac{1}{2}m\sum v_i^{\,2} = \frac{p^2}{2m}$$

$$PE = U(r_i)$$

$$TE = KE + PE$$

$$F = -\nabla PE(r_i)$$

A system of around 1000 atoms is chosen and periodic boundary conditions are applied to the system for it to behave as a bulk material. This means that no surface is considered and the structure repeats in all the three dimensions. From these atomic or molecular level interactions, various properties are then calculated[53]. Out of the different integrators, Predictor-corrector integrator[103,104] was used for the simulations here.

There are various types of ensembles which can be used depending on the requirement. Certain properties can be kept constant while varying the others. In the phase transition calculations it is important to let the volume evolve and not have any constraints on it. Also the pressure should not be allowed to vary and should be kept very low. Some of the different ensembles are as follows:

- Constant Volume - Constant Temperature or Canonical Ensemble: In this type of ensemble: the number of particles (N), the volume (V), and temperature (T) is constant. It is also called as an NVT ensemble

  $$KE = \frac{3}{2} N k_B T$$

- Constant Volume – Constant Energy or Microcanonical Ensemble: In this type of ensemble the number of particles in the system (N), the volume of the system (V), and the energy of the system (E) are all constant. It is also called NVE ensemble.

- Isoenthalpic-Isobaric Ensemble or Constant Enthalpy - Constant Pressure Ensemble: In this type of ensemble the number of particles N, enthalpy H and pressure P are all constant. It is also called the NPH-ensemble.
- The Isothermal–Isobaric Ensemble or Constant Temperature and Constant Pressure Ensemble: In this ensemble temperature T and pressure P are constant. In the NPT-ensemble, the number of particles N is also a constant.
- Constant Temperature–Constant Stress Ensemble: This is constant temperature, constant stress ensemble or isothermal-isotension ensemble[105-107]. In this the number of atoms is also constant. When a system with vacancies or interstitials is being studied for its phase transformation such as melting, the volume of the system is expected to change. There should not be any constraint on the volume as it is very important to let it evolve. Also during this process the pressure values should not be high so that its effect is not prominent. Thus, an isothermal-isotension ensemble gives this flexibility where volume and shape changes but pressure does not. Thus this ensemble is very handy when it comes to studying phase transitions.

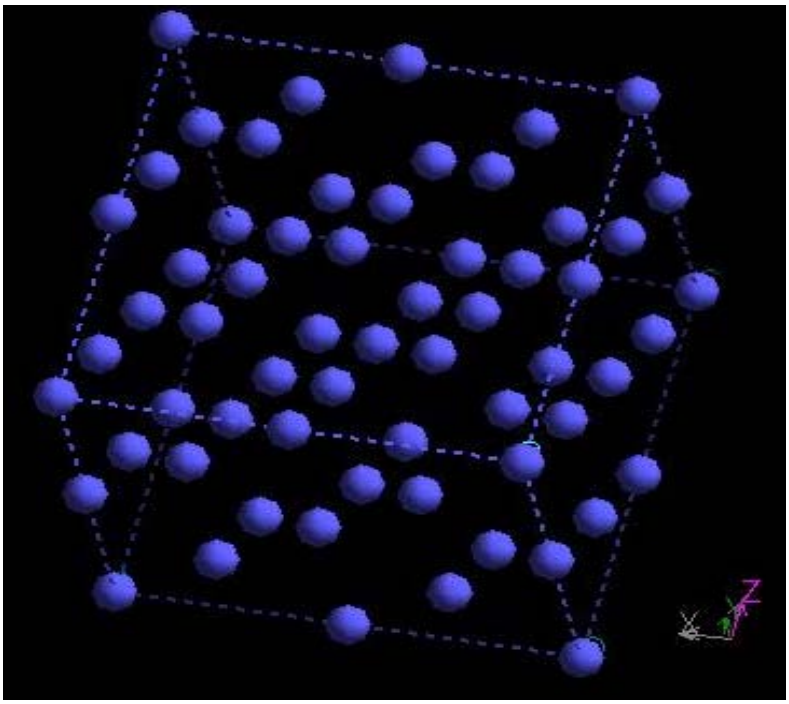

Figure 2: 2X2X2 supercell of copper with a vacancy

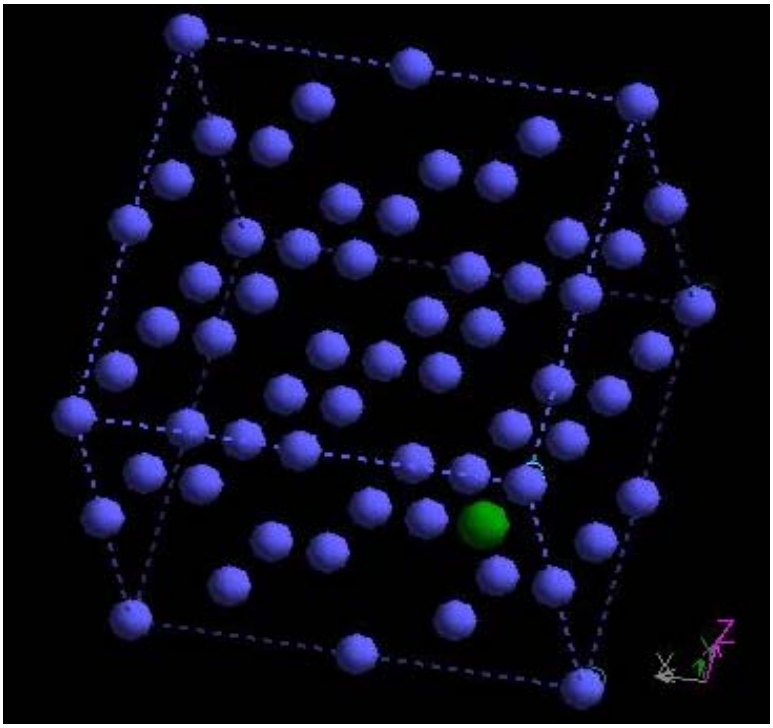

Figure 3: 2X2X2 supercell of copper with an interstitial

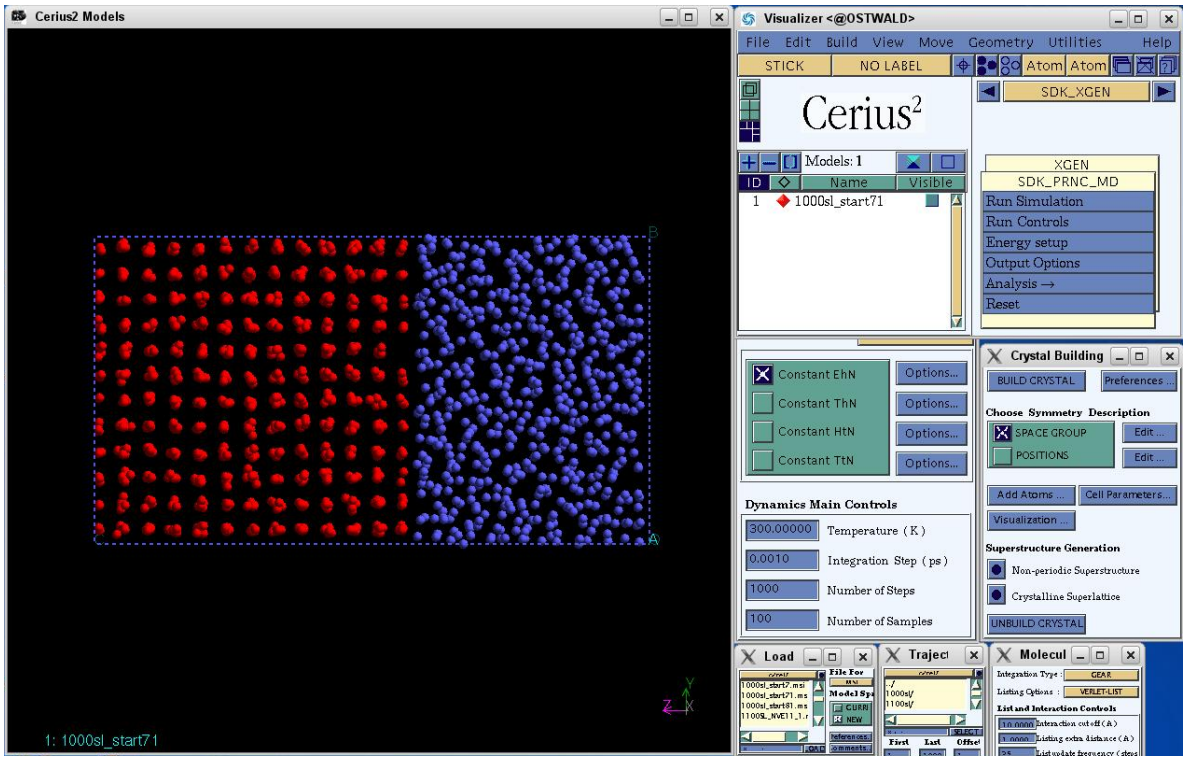

Figure 4: CERIUS^{2TM} developed by Accelerys[108]

CHAPTER III

PROCEDURE

Structures

CERIUS$^{2TM\ 108}$ is used to construct the structures and also to visualize all the simulations. The MD program developed by Cagin[109] is used for our simulations. From a unit cell of copper (fcc) which has 4 atoms as shown in the figure on page 33, a crystalline super lattice is formed, and it consists of 864 atoms of copper. This is done by replicating the unit cell 6 times in each x, y and z directions. Thus there are a total number of 216 unit cells of copper. Three dimensional periodic boundary conditions are applied so as to avoid free surface effects. The 864 atoms of copper is the simulation box which is visualized. The other atoms which will not be seen exist, and are only copies of this simulation box. This the system now behaves like a single bulk crystal. This is taken as an initial structure and single-phase simulations are performed. Copper system of 864 atoms with 0,1,2,4 and 8 vacancies and 1, 2, 4 and 8 interstitials respectively will be formed first.

Vacancy and interstitial: A vacancy is induced by deleting 1 atom out of the 864 atoms of copper, leaving a total of 863 atoms. An example of this is shown in figure 2 for 2X2X2 superlattice of copper. For more vacancies more atoms are deleted, and it is made sure that they are farther apart so as to avoid interaction among them. An interstitial is induced by adding an extra atom between lattice sites, making the system to

a total of 1 atom more than the normal. In this case now there will be a total of 865 atoms when 1 interstitial atom is added. Thus, in the region where the interstitial is present the atoms are crowded and there will be lattice distortions. Figure 3 shows 1 interstitial atom added to a 2X2X2 superlattice of copper. For more interstitials more atoms are added. It is again made sure that these interstitial atoms are kept away from each other so that they do not interact. In this way the system is kept as symmetric as it can be. Since the interstitial system has more atoms, the volume also tends to increase due to this. Figure 4 shows how the interface of CERIUS^2 looks. Figure 5 shows 8 interstitial atoms added to a system of 864 atoms to make a total of 872 atoms. The interstitial atoms are of different color than the normal atoms.

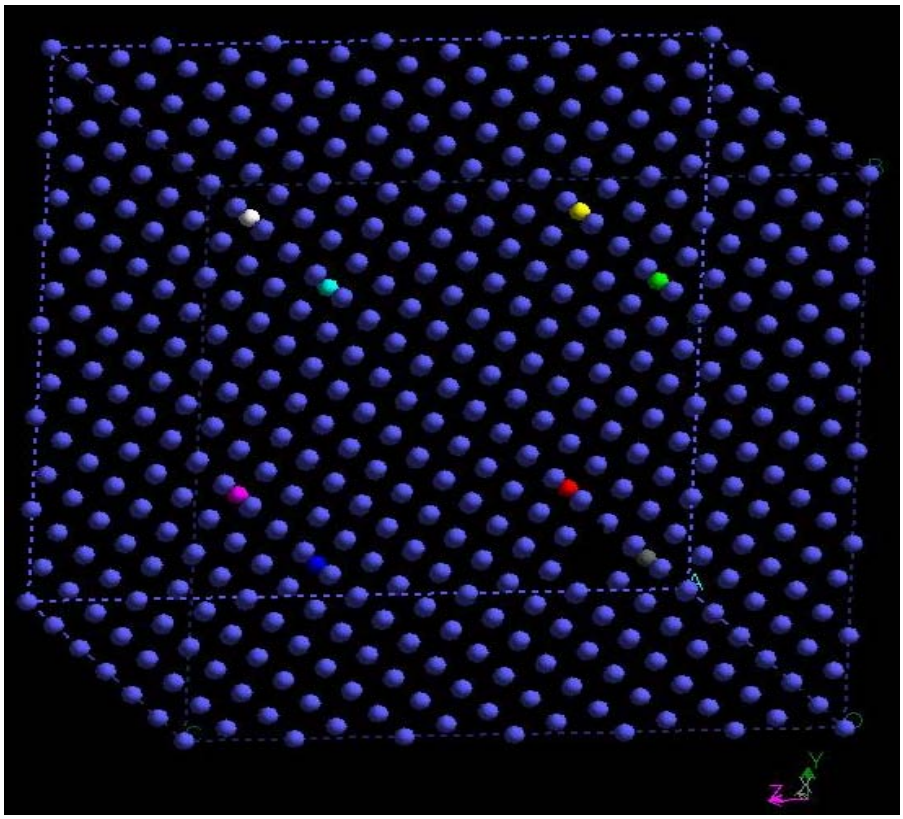

Figure 5: Copper with 8 interstitials (different colored atoms) initial structure

Edge dislocation: In edge dislocation a plane of atoms is missing from their usual lattice sites. To form this first a supercell of 10X10X10 unit cells of copper (4000 atoms) is first constructed. As shown in the figure 6, the whole 11X10 atoms are deleted in (1 1 0) or OA plane. 5 atoms from each end are left and the remaining center part consisting of a total of 110 atoms are deleted and 3890 atoms are remaining. To make the observations easier, the first nearest neighbors of the deleted atoms are red in color and second nearest neighbors are green in color.

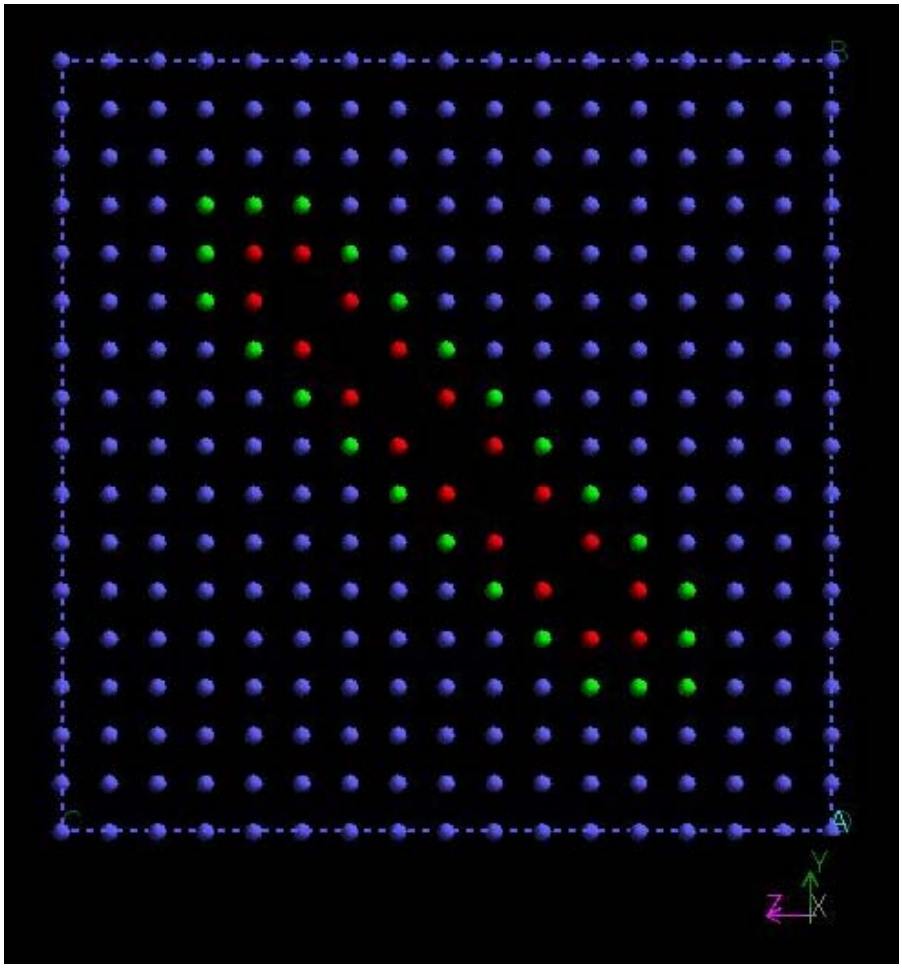

Figure 6: Copper edge dislocation

Grain boundary: Two different types of grain boundaries are constructed using Grain Boundary Studio (GB Studio)[110]. The coordinates of atoms are obtained from GB Studio for these systems and then these coordinates are used in CERIUS^2 to perform simulations. The figures of grain boundaries shown here are formed in CERIUS^{2TM} using the coordinates obtained from GB Studio. Figure 7 shows an interface of GBStudio.

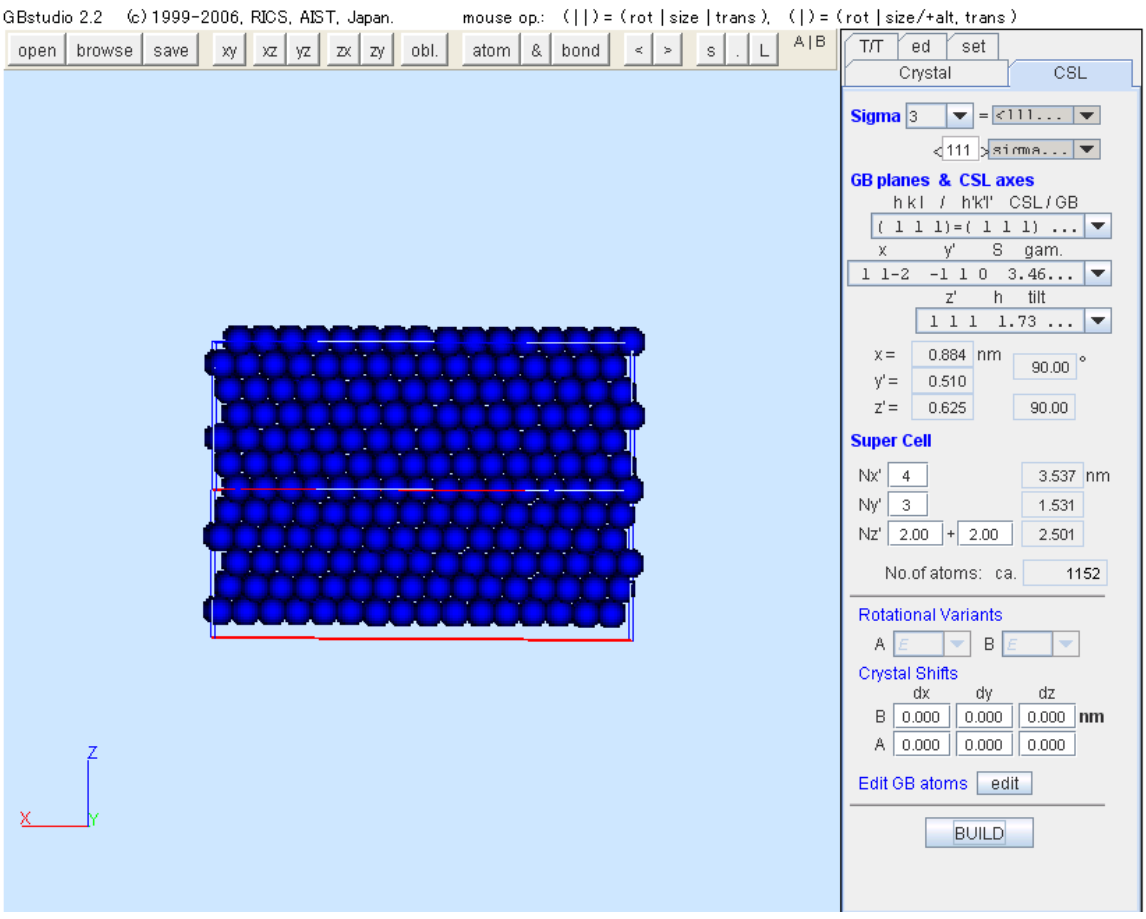

Figure 7: GB STUDIO interface [110]

The first structure is Sigma3, <111>, 60.0. A crystalline superlattice of copper with a grain boundary with 1152 atoms is formed. This is formed when the unit cell is extended 4 times in X-direction, 3-times in Y-direction and 2+2 times in Z-direction. 2+2 signifies that the grain boundary is in Z-direction half way through the lattice and parallel to XY-plane. This grain boundary structure can be seen in figures 8. The atoms are colored at the grain boundary so that they can be observed.

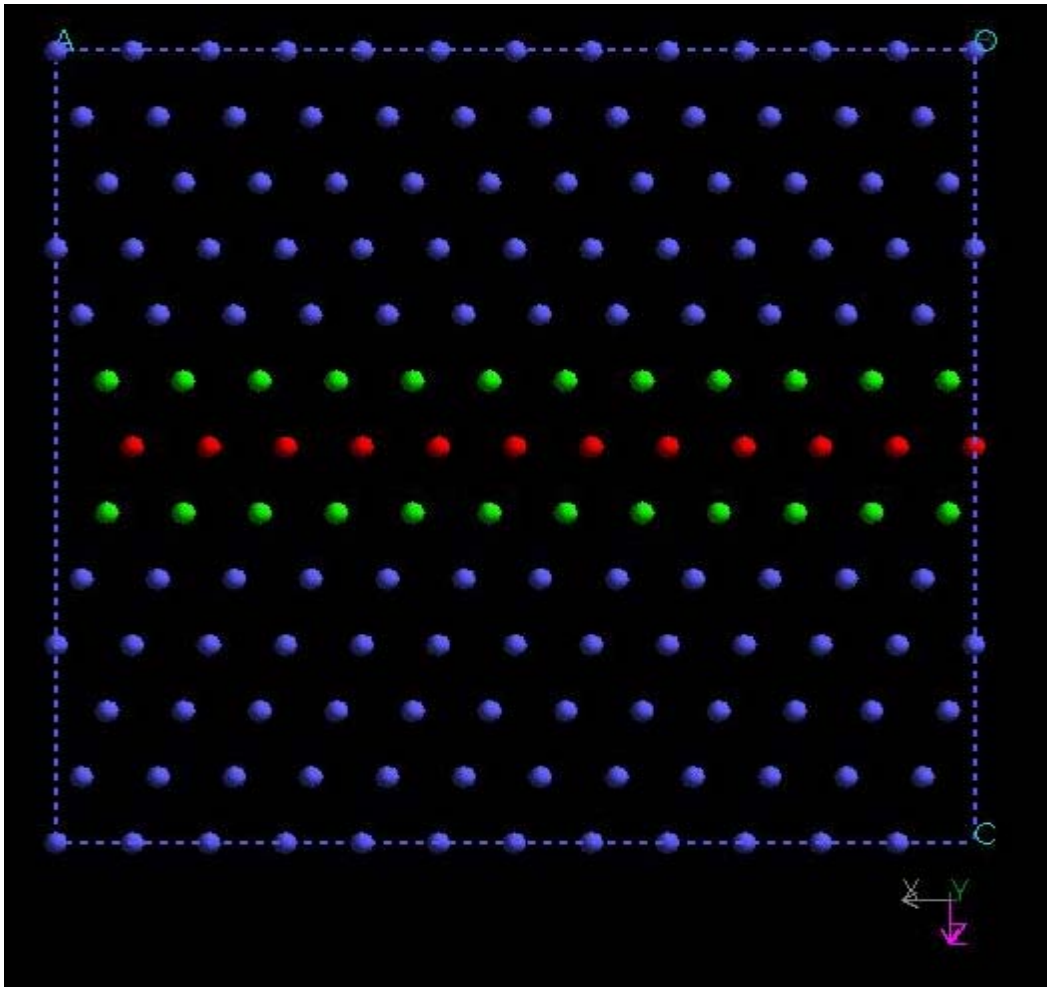

Figure 8: Grain boundary structure 1: Sigma 3, <111>, 60^0

The second structure is Sigma5, <210>, 180.0. A crystalline superlattice of copper with a grain boundary with 960 atoms is formed. This is formed when the unit cell is extended 4 times in X-direction, 3-times in Y-direction and 2+2 times in Z-direction. 2+2 signifies that the grain boundary is in Z-direction half way through the lattice and parallel to XY-plane. This grain boundary structure 2 can be seen in figure 9. The atoms are colored at the grain boundary so that they can be observed. This type of grain boundary system is highly mismatched at the boundary.

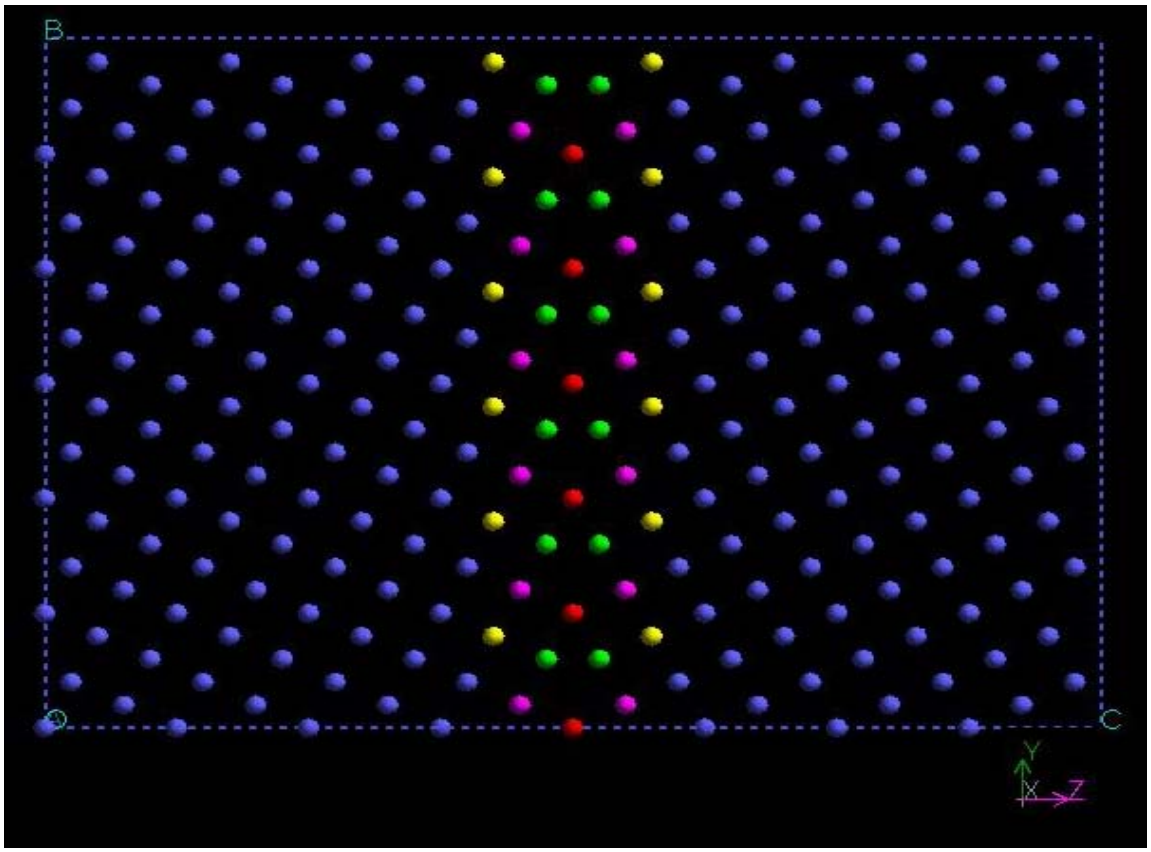

Figure 9: Grain boundary structure 2: Sigma 5, <210>, 180^0

Phase-coexistence simulation: Since the melting point obtained using single phase simulation is the upper limit of melting, phase-coexistence simulations are done so as to get the true melting point of the system. The structure needed for two-phase simulation is constructed using CERIUS^2. The two-phase simulation structures are needed at various temperatures ranging between the two phase transitions points (melting point and freezing point) obtained using the single phase simulations. Thus construction of structure at each temperature requires the similar procedure with different inputs. Procedure to construct a structure will be described for the particular case of 1200K. The final structure would be obtained by putting together a solid and a liquid structure. It is first required to obtain the solid structure and the liquid structure separately, using the single phase simulations. It should be made sure that these two structures are finally at 1200K. There are some important points that should be kept in mind during the whole process. The main aim is to construct an interface of the two phases. This interface should be same for the two structures, meaning the interface area of the solid structure and that of the liquid structure needs to be of the same dimensions so that there is no mismatch.

Solid: The solid structure needed at 1200K should have the same volume that the solid had while performing the single phase simulation using TtN ensemble for pure copper. Thus, the volume of the solid at 1200K is noted from single phase a simulation that was done earlier. Let this be V_{1200}. Thus, if a_{1200} is the lattice parameter that would be required as a starting point to get the solid structure, then,

$$a_{1200}(solid) = \frac{\left(V_{1200}^{1/3}(solid)\right)}{6}$$

Now, taking a_{1200} as the lattice parameter, a 6X6X6 supercell of copper is constructed. This is heated slowly until 1200K using the NVT ensemble. This ensemble is used so that the interface is intact. Thus the interface is a_{1200} X a_{1200}.

Liquid: The interface of the liquid structure needs to be the same as that of solid. But a liquid phase with same number of atoms would occupy a larger volume compared to a solid structure since density of liquid is lower than that of solid. Thus the liquid structure is formed using less number of atoms. A 5X5X6 superlattice of copper atoms is formed. Thus $5a_{1200}$ X $5b_{1200}$ interface of liquid is same as $6a_{1200}$ X $6b_{1200}$ interface of solid. Also, the c value of the liquid is calculated from the expression of volume, where volume is taken as the volume of the melt that had been obtained from single phase simulation. Thus the following expressions are obtained:

$$a_{1200}(solid) = b_{1200}(solid) = c_{1200}(solid)$$

$$a_{1200}(liquid) = \frac{6}{5} a_{1200}(solid)$$

$$b_{1200}(liquid) = \frac{6}{5} b_{1200}(solid)$$

$$V_{1200}(556 - liquid) = \left(\frac{5*5}{6*6}\right) V_{melt}(666 - liquid)$$

$$c_{1200}(liquid) = \frac{V_{1200}(556 - liquid)}{6*\left(5a_{1200}(liquid)\right)*\left(5b_{1200}(liquid)\right)}$$

These are the lattice parameters that would be finally used to construct the liquid structure. From this initial structure the supercell is constructed and heated until the structure melts keeping the volume constant. After the structure melts, the melt is again equilibrated at constant volume to 1200K and it is made sure that the pressure is low.

After the solid and liquid structures are obtained separately, they are brought together and placed side by side so as to match their common interface as shown in the figure 10. The atoms from the solid structured are colored red so that their movement can be observed and they can be distinguished from the other liquid atoms. Three dimensional periodic boundary conditions are applied to the overall structure. Thus it is made sure that the atoms at the left and right ends of the box shown in figure 10 are not close to each other and there is a small gap between them. Also at the center of the box in figure 10, at the solid liquid interface there should be an interfacial thickness. This is provided so that the solid and the liquid atoms at the interface do not repel because of the close proximity between them.

Some trial and error has to be done to make sure that the atoms at the interface are not to close or not to far from each other. This procedure is repeated to get solid liquid structure at various temperatures between the upper and lower limit of phase transformation temperatures.

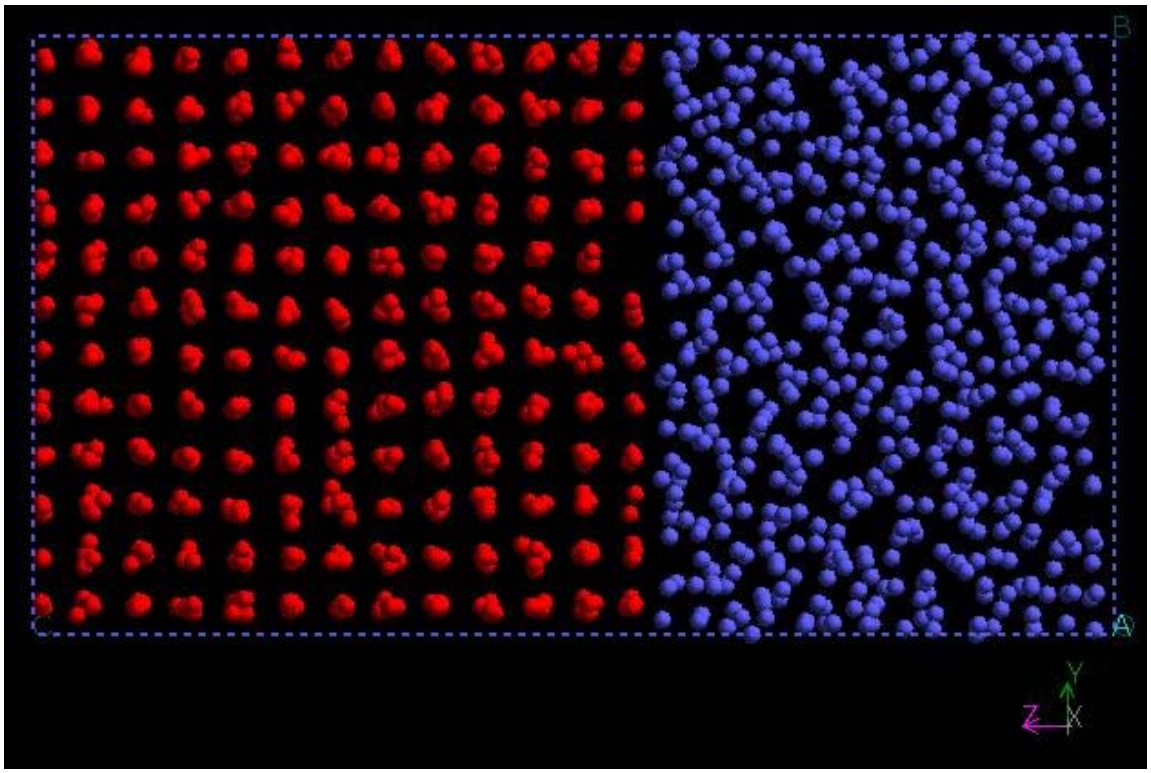

Figure 10: Copper liquid-solid interface for two-phase simulation

Previous researchers have used very simple pair potentials, or sometimes even three body potentials, which is not how atoms interact in real crystals. Many-body interactions have to be taken into account for metals. Most of the potentials used by previous researchers were short ranged which is not the case in real crystals. If long range interaction is considered as not important then a lot of computational cost can be reduced, but the calculations are a lot inaccurate[111]. Hence a more accurate potential is chosen, which has already been tested earlier and proved to be a good match for metals in consideration.

Quantum Sutton Chen potential

Here Sutton-Chen (SC) many body potential [112] with quantum corrections (QSC) [113] is used, which is moderately long-ranged. Some calculations using this have been done on PD-Ni alloys[114-116] and other systems [117-122]. Very accurate results have been obtained using this potential and hence it is chosen for the simulations. The equations for the same are given below. We write the equation for the total potential energy as,

$$U_{tot} = \sum_i U_i = \sum_i [\sum_{j \neq i} \frac{1}{2} \varepsilon_{ij} V(r_{ij}) - c_i \varepsilon_{ij} (\rho_i)^{1/2}]$$

In the above equation, $V(r_{ij})$ is a pair wise potential which describes long-range interaction between atoms *i* and *j*.

$$V(r_{ij}) = (\frac{a_{ij}}{r_{ij}})^{n_{ij}}$$

and ρ_{ij} is a local energy density term which accounts for the cohesion associated with atom *i* and is given by

$$\rho_i = \sum_{j \neq i} \phi(r_{ij}) = \sum_{j \neq i} (\frac{a_{ij}}{r_{ij}})^{n_{ij}}$$

In the above equations, Here r_{ij} is the distance between atoms *i* and *j*, *a* is a parameter with dimensions of length, *c* is a positive dimensionless parameter which scales the cohesive term relative to attractive term, ε sets the overall energy scale, and n and m are positive integer parameters such that n>m.

Table 1: Parameters for the SC and QSC many-body potential for Cu

	n	m	ε (eV)	c	a (Å)
QSC[113]	10	5	0.0057921	84.843	3.603
SC[123]	9	6	0.0123820	39.432	3.610

H. H. Kart and coworkers calculated thermal and mechanical properties of both pure elements and ordered systems at low and high temperatures and found that the Q-SC parameter results are closer to experimental data than the SC results. This indicates that the Q-SC potential produces more accurate results at higher temperatures[124]. The predictor-corrector algorithm of Gear was used to solve the equations of motion[103,104]. The SC and QSC parameters for copper are listed in Table 1.

Single phase simulations

Earlier single-phase simulation were seen to produce decent results at low pressures, whereas at high pressure there was some amount of superheating observed[52]. Simulations are done for constant stress–constant temperature ensemble [105-107] using the MD program developed by Cagin[109]. All simulations are done at 0 pressures. A total number of 50000 steps are used for each simulation. The time step used was 0.001ps. Copper system of 864 atoms with 0,1,2,4 and 8 vacancies and 1, 2, 4 and 8 interstitials respectively was used. Before any simulation is done, the energy of every system is minimized so as to get a stable configuration of the structures. A supercell and a unit cell of copper are shown in figure 11 and figure 12 respectively.

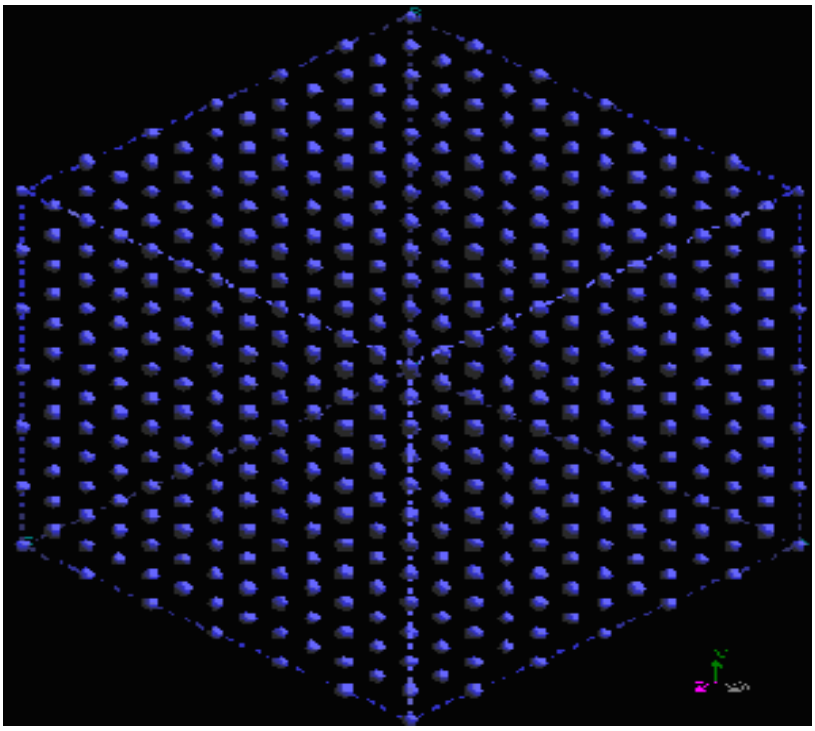

Figure 11: Supercell of 864 atoms of Cu

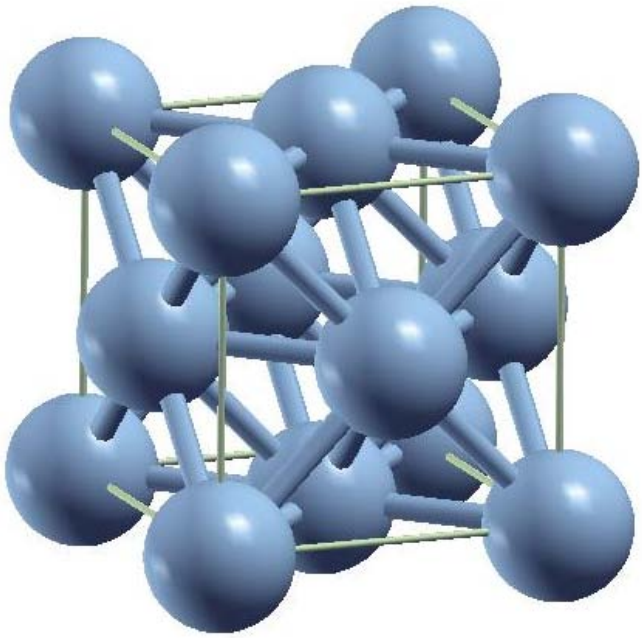

Figure 12: Unit cell of Cu (FCC) created using XCrySDen [125-127]

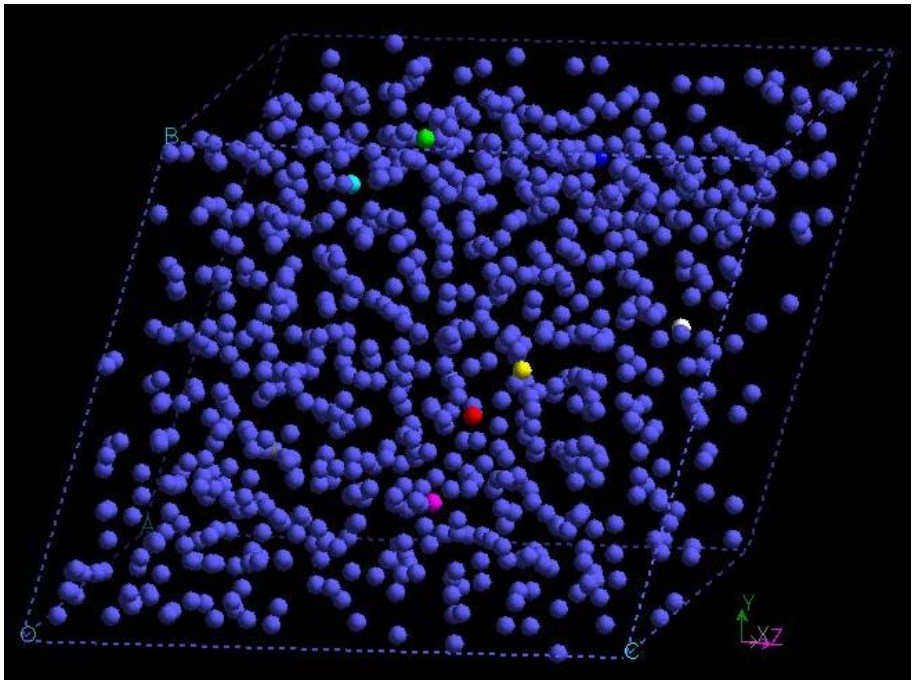

Figure 13: Copper with 8 interstitials at 1600K

At the end of each heating and cooling step, physical properties like pressure (P), density (d), specific heat capacity (Cp), average kinetic energy (K.E), average potential energy (P.E), average total energy (T.E) and their fluctuations are observed. The temperature is increased from 300K with an increment of 100K each time the melting transition is observed. Drastic change in volume and other properties signifies melting of the crystal. The heating rate used is 2 K/ps. It is important to give enough simulation time for the system to reach equilibrium. Now a temperature below the transition temperature is selected and this time the temperature increment is kept 20K keeping other parameters same so that the heating rate is slower. This is done till the phase transition takes place and the structure will melt as shown in figure 13. The phase

transformation temperature has been narrowed down. Again the same procedure is repeated now with 5K increments. Using this method the range of phase transformation is narrowed down to 10K. Thus the melting temperature is obtained. This is the upper limit of melting temperature considering it has gone through some amount of superheating.

To get the freezing curve and freezing point, the melt structure is taken and the system is cooled slowly until it refreezes. Again near the freezing point, cooling rate is decreased so as to narrow down the range of freezing point. The freezing point thus obtained would be the lower limit to the freezing point as it has gone through some amount of supercooling. The actual

Thus a plot of density versus temperature at constant pressure can be obtained from the runs, and the temperatures at the first-order phase transitions (melting and freezing) are obtained. It can be identified that the system has melted by observing how the various properties vary according to temperature. This observed melting point may not be the true melting point, since the system might be in a superheated condition. When the system temperature is decreased from the melt gradually the system freezes at some point. This again might not be the true freezing temperature as the system might be supercooled. The figure for the melting-refreezing hysteresis is plotted which shows: the system usually undergoes superheating before melting and supercooling before refreezing.

The same procedure is repeated for edge dislocations and grain boundaries. Grain boundary loops have not been considered. Also, interaction of grain boundaries with point defects such as vacancies and interstitials is also not considered.

Phase-coexistence simulations

There are several methods to study phase coexistence. One of them is Gibbs ensemble method[128-131]. This method becomes ineffective when one of the two phases becomes very dense. Another method to study phase-coexistence is Gibbs-Duhem integration method of Kofke[132-134]. This requires just one point on the coexistence curve to be known. From that the rest of the curve can be obtained. Some of the other methods are covered in Ref.[135]

Two-phase simulations are performed to calculate the true melting point of the crystal. The single phase simulations just provide the upper and low limits to the phase transformation temperatures and two-phase simulation is a well known method to overcome this problem of hysteresis. The solid and liquid structures are obtained from the single phase simulation and then brought together to form the solid liquid interface structure as described earlier. After the structure is constructed at a particular temperature, constant temperature–constant stress simulations are done at that temperature. This way the pressure is kept constant and the volume is allowed to change. The system is observed with time. If the solid atoms near the interface start disordering into a liquid melt, it means that the temperature at which the current simulations are being done is above the melting temperature. This is the reason even the solid is starting

to melt. In this case, another temperature is chosen which is below this temperature. Simulations are done at the new temperature taking the solid liquid interface structure that was constructed at the new temperature. Suppose this time the liquid atoms near the interface start to arrange themselves in an orderly fashion giving a hint that the liquid structure is actually solidifying, it means that this new temperature that was chosen is lower than the melting temperature. Hence the system is freezing. Thus, the third temperature to be chosen should be above the second temperature but below the first temperature that was chosen. This is repeated until the temperature at which the solid continues to behave as a solid and the liquid continues to behave as a liquid. This would be the true melting temperature.

CHAPTER IV

RESULTS AND DISCUSSION

Single phase simulations

Single phase simulations are done for the various systems of copper with and without defects as mentioned earlier. This includes copper with 0, 1, 2, 4 and 8 vacancies and 0, 1, 2, 4 and 8 interstitials, edge dislocation and also grain boundaries. For each of these systems the temperature is increased slowly until the system melts. Various properties of the system are recorded for each simulation. The melt structures are then cooled slowly until the structure freezes. Table 2 shows the linear expansion of copper with no defects as the temperature increases. The values obtained in this work using Quantum Sutton Chen potential are compared with those calculated by Sutton Chen potentials[123] and experiment. Values of QSC are closer to experiment than that of SC. Also, as the temperature increases, both SC and QSC values are farther from the experimental values.

Table 2: Linear expansion of copper as a function of temperature

	500K	750K	1000K
SC[a]	0.58	1.4	2.42
QSC[b]	0.54	1.24	2.04
Experiment	0.34	0.82	1.36

[a] Ref[123]

[b] This work

The density of copper at 300K as calculated here using QSC (8.9958 g/cm^3) is closer to the experimental value (8.912 g/cm^3) than that obtained using SC potential (8.7235 g/cm^3) in Ref.[123]. Figure 14 is a typical graph of MD temperature against time during melting. Figure 15 and figure 16 show the potential energy and total energy during melting as time progresses. These graphs are obtained for the simulation that was done to increase the temperature from 1355K to 1360K. This is when the phase transition occurs from a solid phase to liquid phase. This can be observed from these time graphs. As the MD time progresses the average temperature approaches the final value of 1360K. The total energy starts increasing rapidly around 35ps until about 40ps. This is the period where the phase transition takes place. The potential energy shows a similar behavior to total energy, showing a drastic increase between 35ps to 40ps.

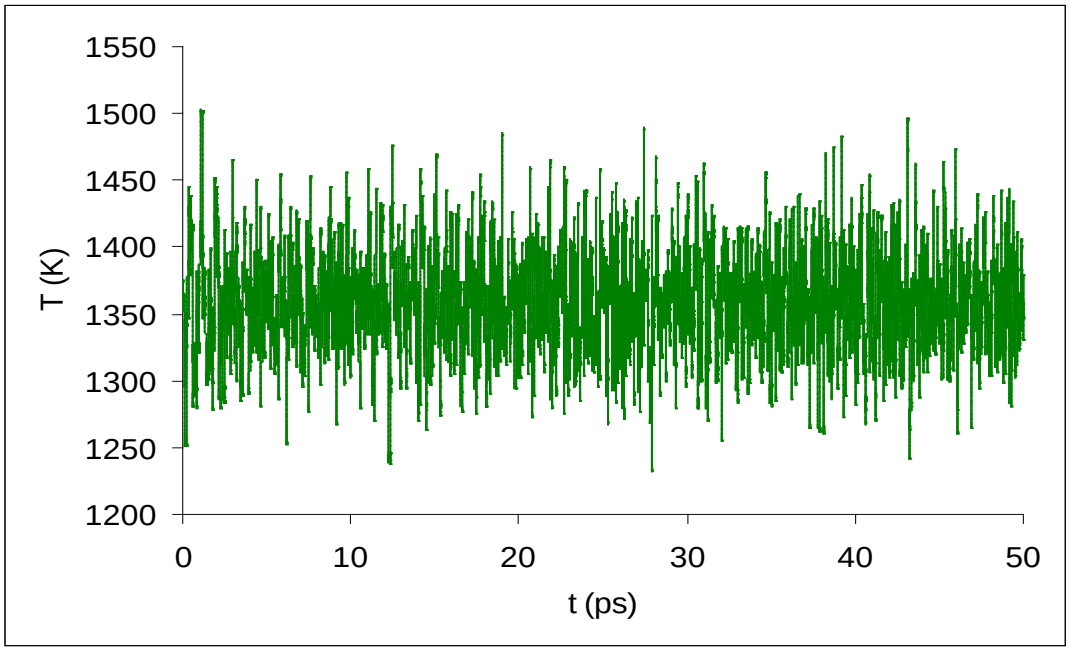

Figure 14: Temperature Vs time for copper without defects at 1360K

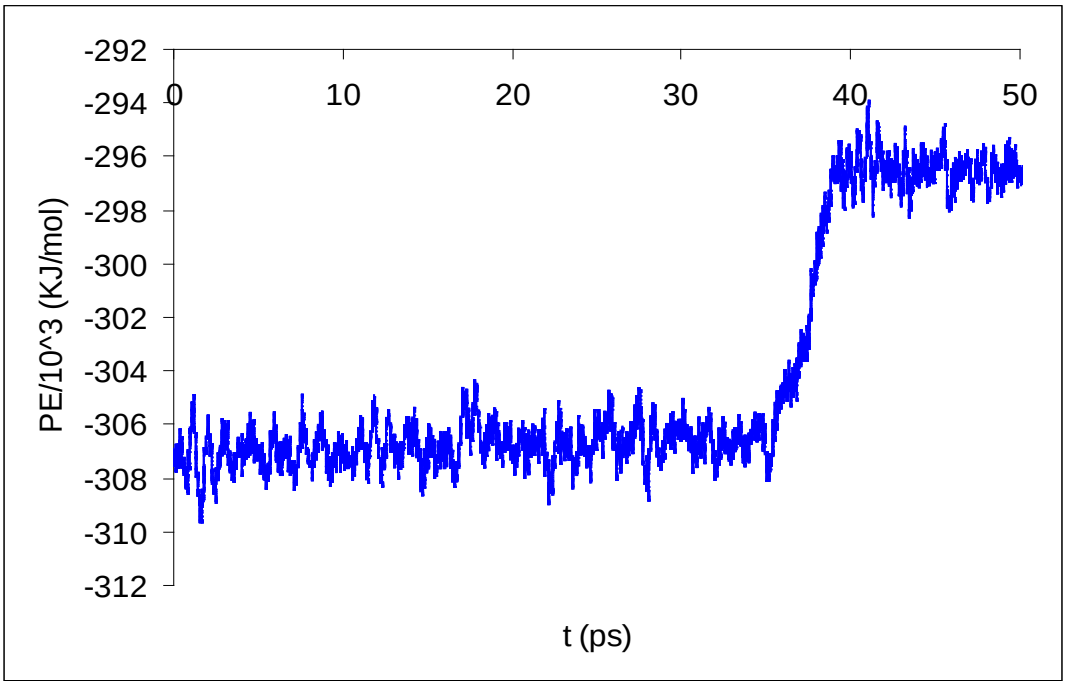

Figure 15: Potential energy Vs time for copper without defects at 1360K

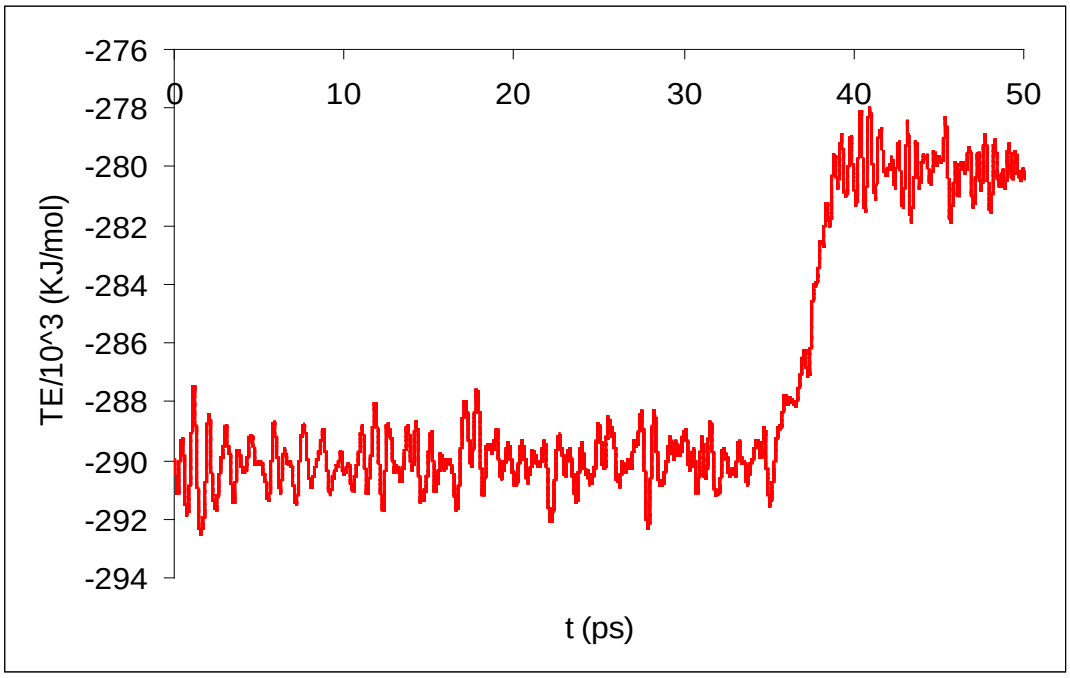

Figure 16: Total energy Vs time for copper without defects at 1000K

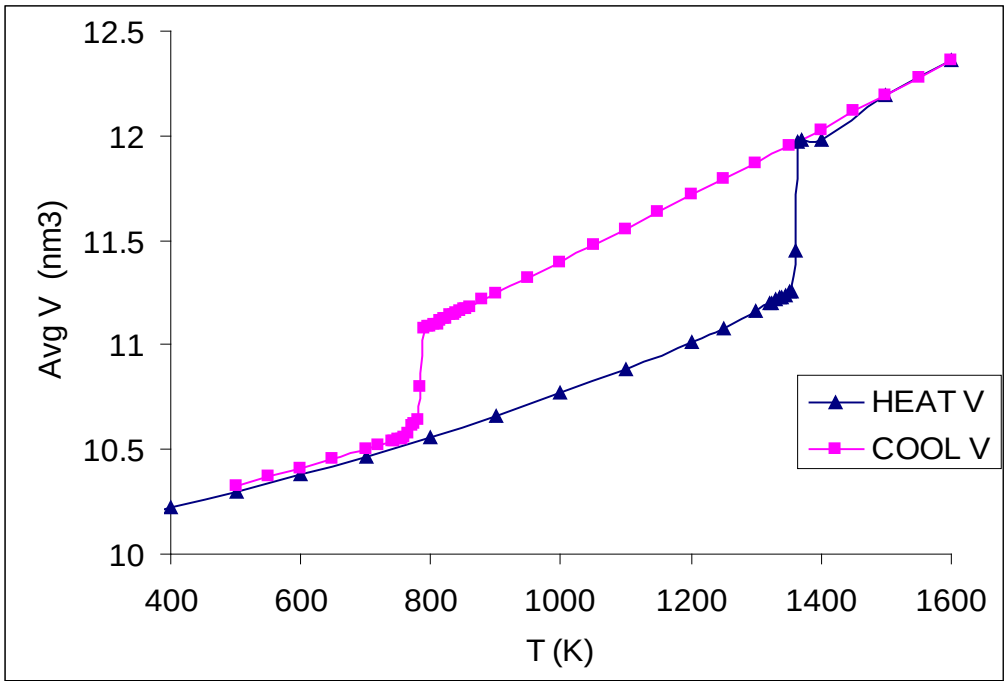

Figure 17: Average volume Vs temperature for copper without defects

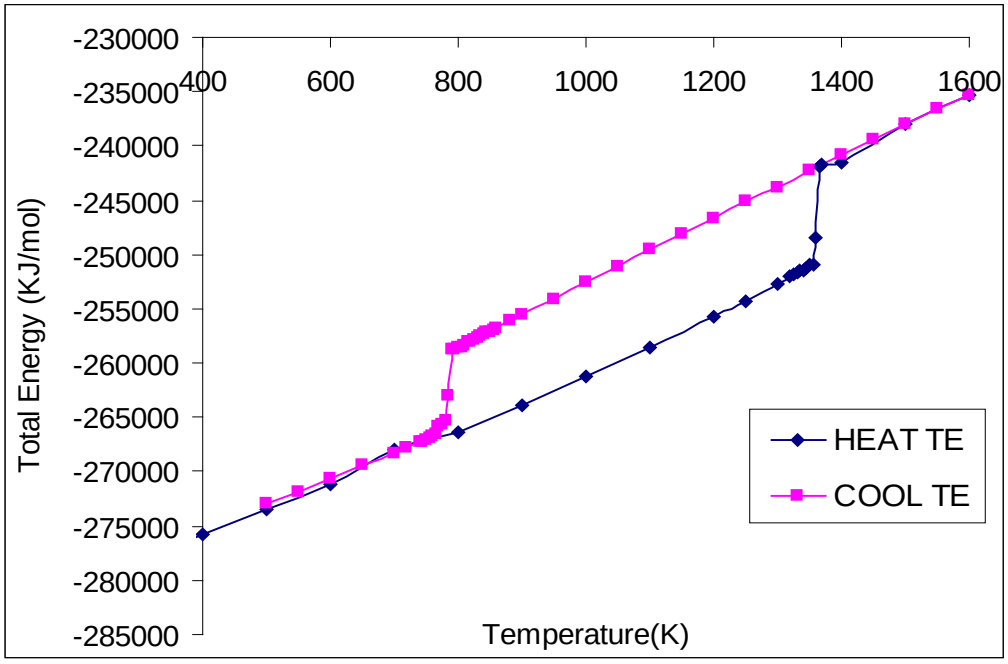

Figure 18: Total energy Vs temperature for copper without defects

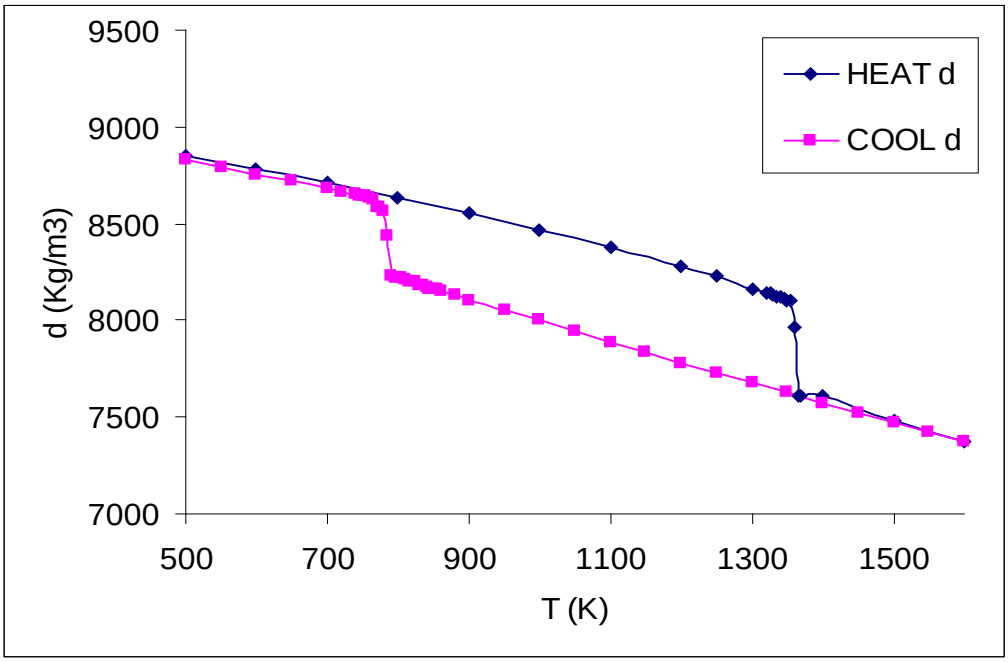

Figure 19: Density Vs temperature for copper without defects

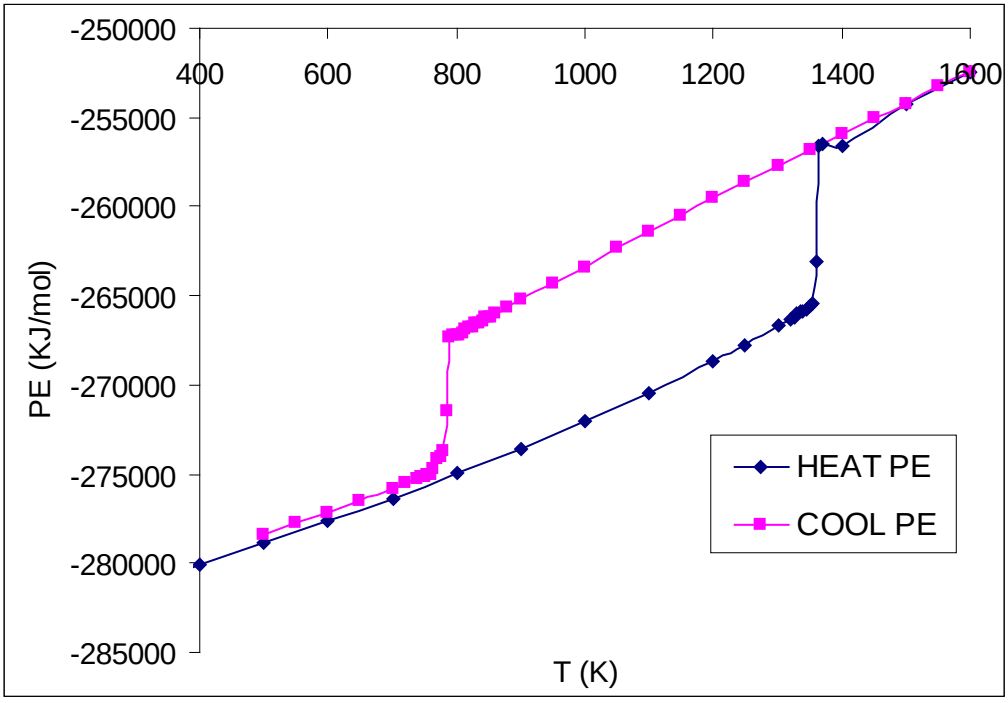

Figure 20: Potential energy Vs temperature for copper without defects

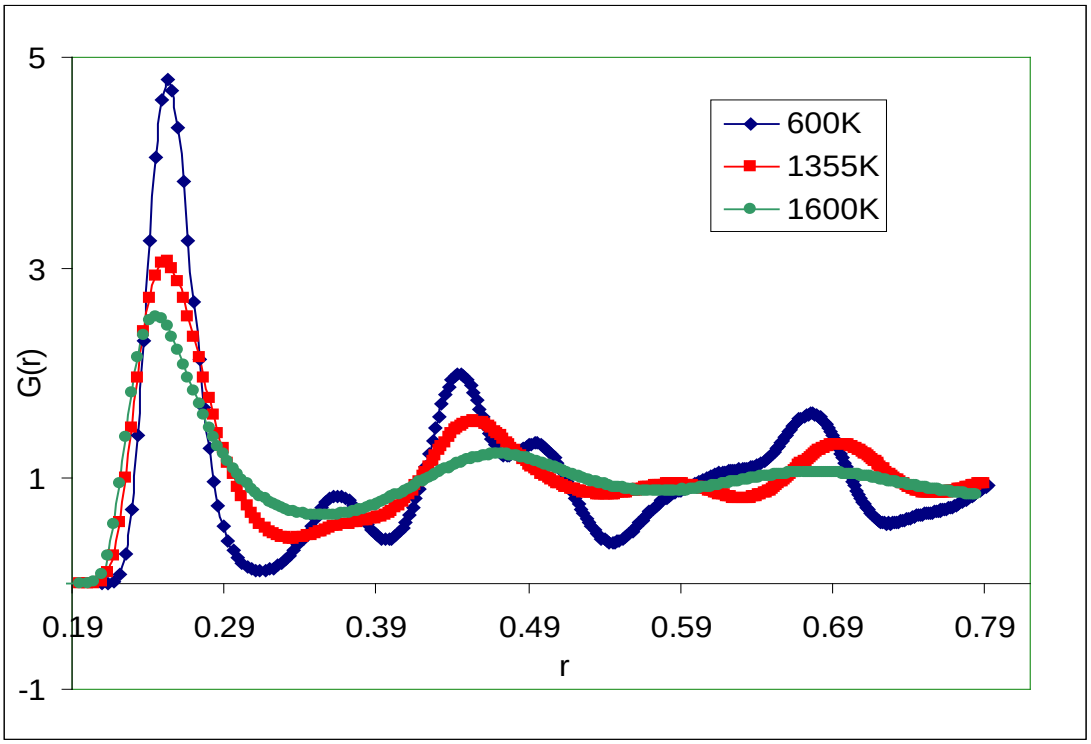

Figure 21: Radial distribution function at 600K, 1355K and 1600K for Cu without defects

Various properties like volume, density, total energy, potential energy, kinetic energy and heat capacity for defect-free copper crystal are studied. The curves for the copper with defects and vacancies are qualitatively similar to these. From figure 17 it can be seen that volume varies linearly with temperature up to a certain point, then makes a jump and then again is linear. Similar pattern is followed by total energy as shown in figure 18. From figure 19 it is seen that the density follows opposite pattern than the volume curve because density decreases when phase transformation takes place from solid to liquid. Also in figure 20 potential energy follows same pattern as kinetic energy. Figure 21 shows the radial distribution curve for copper without defects at 600K when it is a solid, 1355K when the solid is melting, and 1600K when it is a liquid. It can

be seen that the first peak is high at 600K indicating that the system is a solid. At 1355K the height of the first peak decreases and also the second peak disappears indicating that the system is melting. Figure 22 shows that the kinetic energy increases linearly with temperature. The heat capacity curve shows a sharp peak at the phase transformation points as shown in figure 23. The phase transformation does not occur at a single point but occurs in a range of temperature. This is due to the fact that the melting starts at a point and then spreads slowly until the whole system melts. In our calculation the copper structure shows a melting point of 1360 ± 5 K, this is written because the melting occurs in the range 1355-1365K. Also this temperature is an upper limit to melting temperature as it is more than the true melting point. The system might be in a superheated state. After further heating the system to higher temperatures and then when the melt structure is cooled slowly, it does not solidify in the range it had melted. It remains in liquid state until 780-790K, where it solidifies. This is mainly because of supercooling. The actual melting temperature might be somewhere between these two transition temperatures. The true melting is later found from two-phase simulations. Graphs for various properties against temperature are shown below. It can be seen that volume, total energy and potential energy show a similar behavior. Density on the other hand decreases when it goes from solid to liquid.

When the system is in heated state at any temperature below the melting point, although the atoms fluctuate from the initial position but one can still observe some kind of pattern. Once the crystal melts the pattern disappears indicating the phase transition and which can be seen from the homogeneous liquid structure.

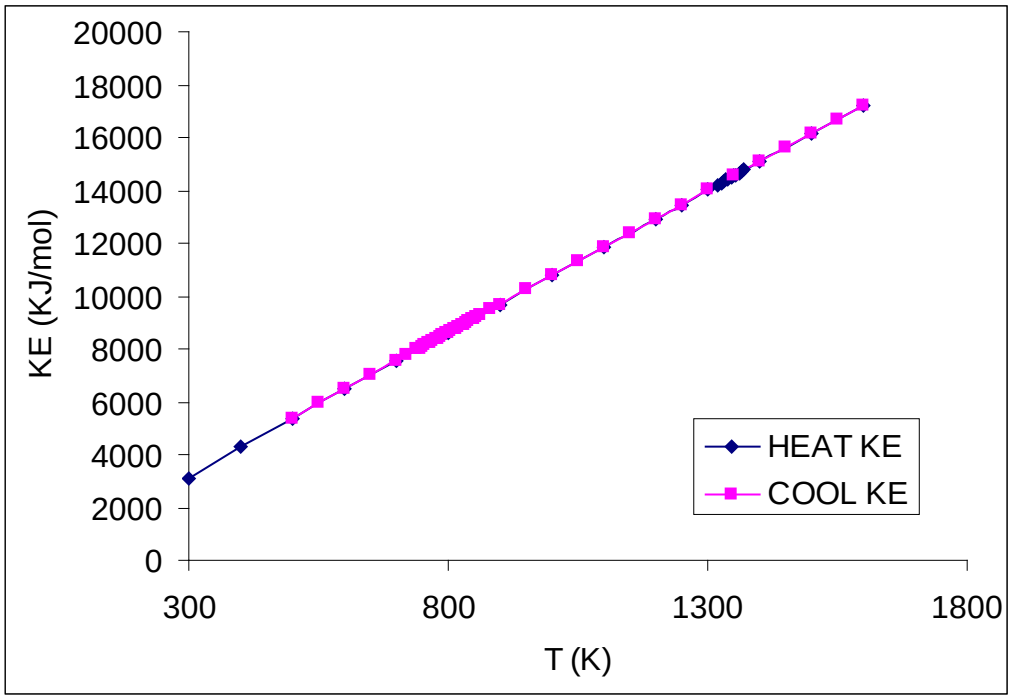

Figure 22: Kinetic energy Vs temperature for copper without defects

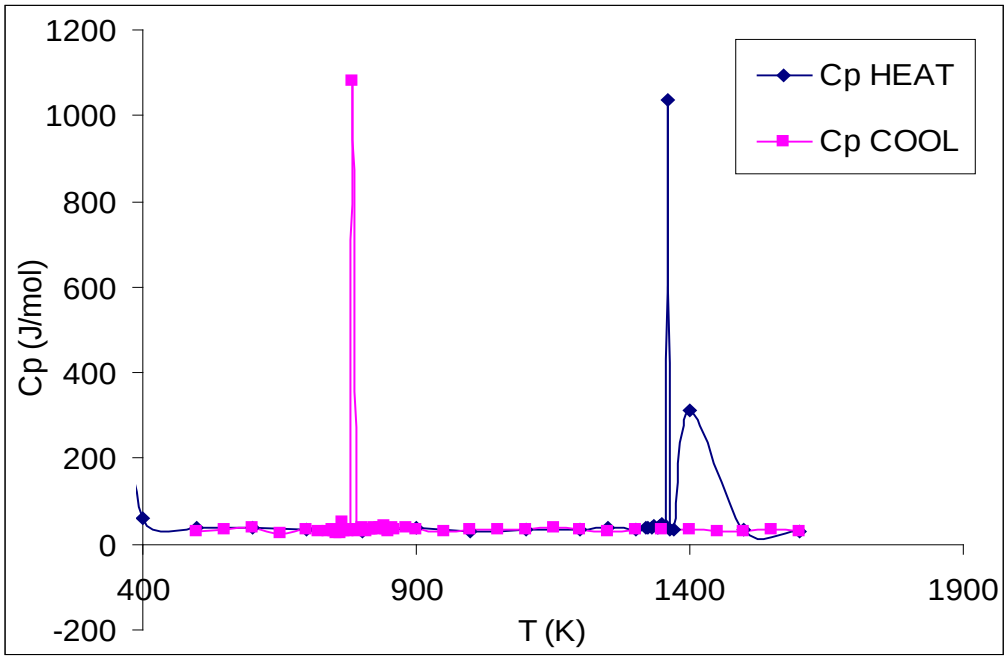

Figure 23: Heat capacity Vs temperature for copper without defects

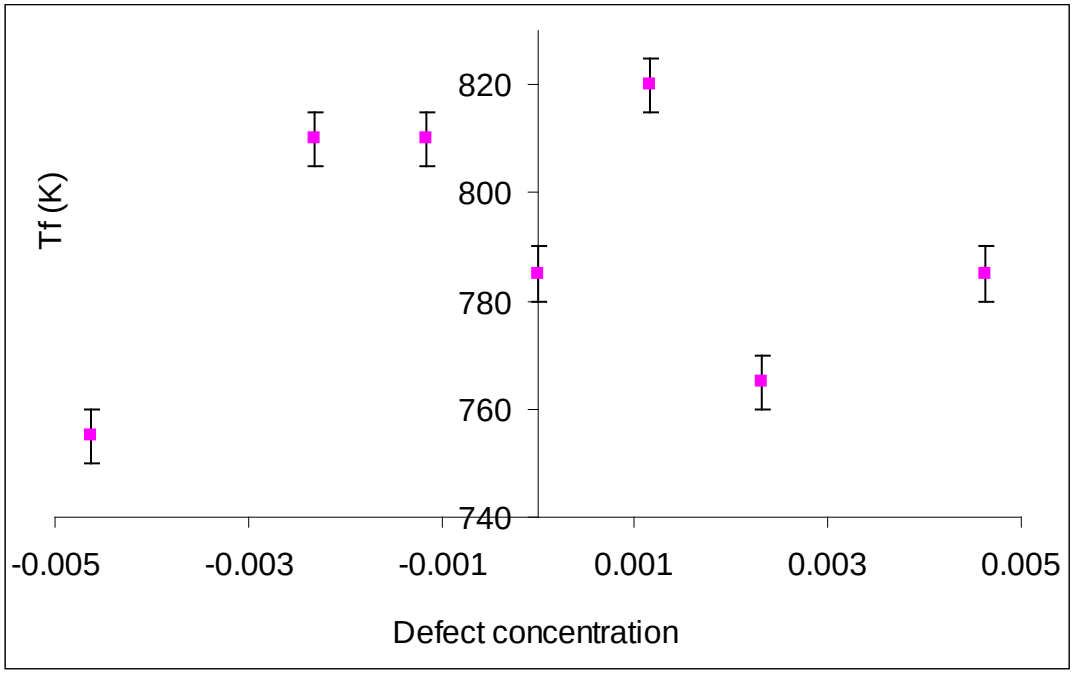

Figure 24: Freezing points Vs number of defects

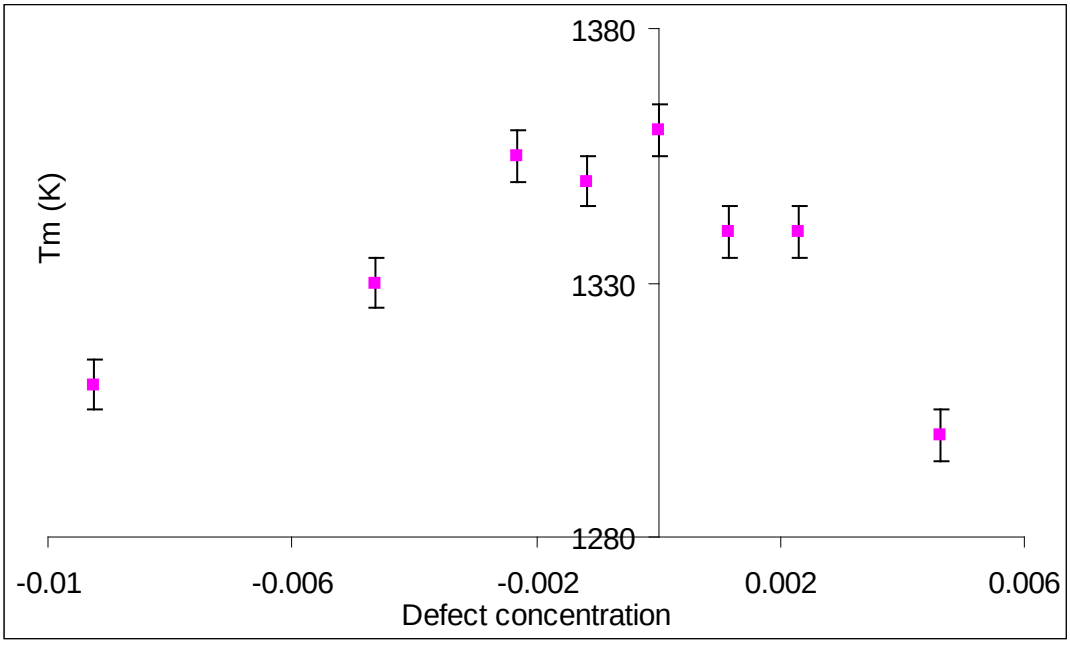

Figure 25: Melting point Vs number of defects

Vacancies and interstitials: From figure 24 we can see that the freezing point does not follow a fix pattern with variation of number of point defects. From figure 25 we can see that the melting points decrease as the number of vacancies increase. This might be because there are fewer bonds when there are vacancies. For interstitials we see that the melting point decreases as number of defects increases. This can be explained by the fact that interstitials cause instability in the structure of a crystal. Since the interstitial system has more atoms, the volume also tends to increase due to this. Figure 26 shows the fractional increase in lattice parameter with increase in defect concentration. For vacancy there is a very small decrease in lattice parameter, whereas for interstitial concentration of around 1% there is almost 1% increase in lattice parameter.

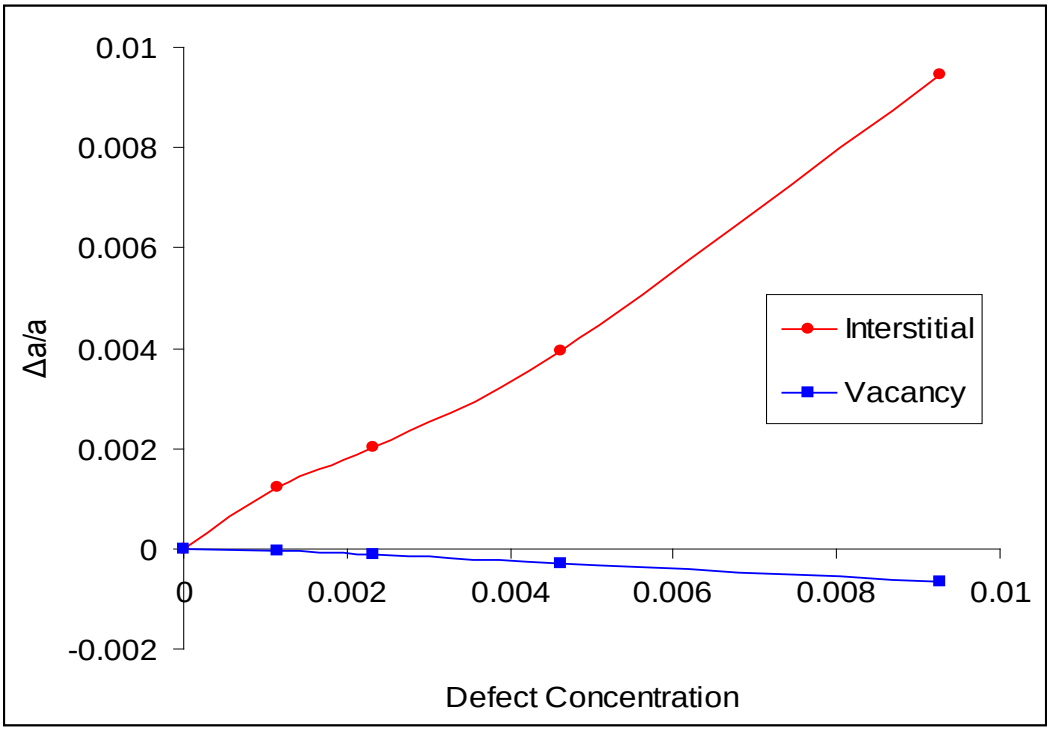

Figure 26: Fractional increase in lattice parameter Vs concentration of point defects at 300K

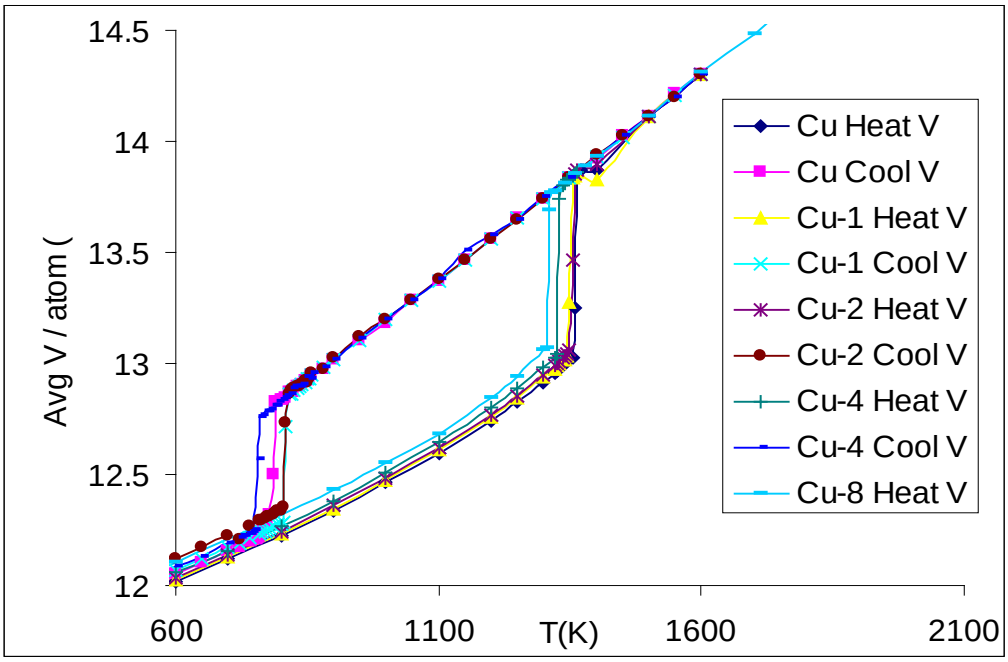

Figure 27: Average volume per atom Vs temperature for Cu with 0, 1, 2, 4 and 8 vacancies

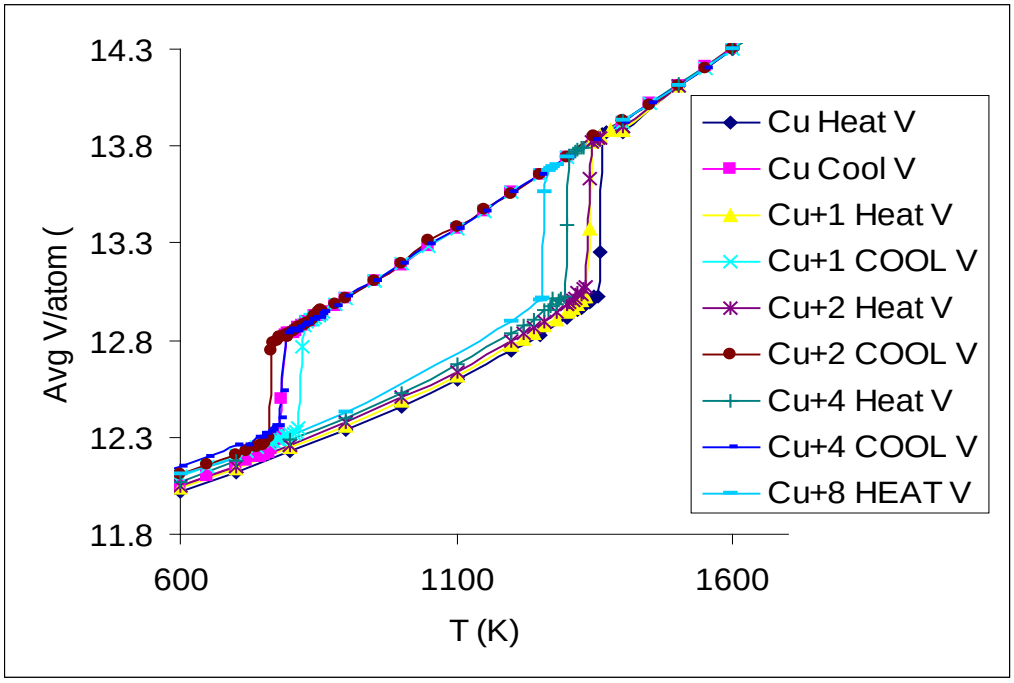

Figure 28: Average volume per atom Vs temperature for Cu with 0, 1, 2, 4 and 8 interstitials

Figure 27 shows the variation of average volume per atom with temperature for all the systems of copper with vacancies and figure 28 shows the same for interstitials. It can be seen that all the systems of copper show a similar hysteresis behavior with a small difference in the phase transformation points. In case of vacancies, the volume does not seem to change a lot and the curves for various numbers of vacancies seem to overlap. But in case of interstitials there is a change in volume due to lattice distortions; hence the volume curves do not overlap for various numbers of interstitials.

Table 3: Melting and freezing points of copper with various number of defects

#Defects/N	#Defects	System	T_m (K)	T_f (K)	T_m - T_f (K)
-0.0093458	-8	Cu-8	1310 ± 5 K		
-0.0046512	-4	Cu-4	1330 ± 5 K	755 ± 5 K	575
-0.0023202	-2	Cu-2	1355 ± 5 K	810 ± 5 K	545
-0.0011587	-1	Cu-1	1350 ± 5 K	810 ± 5 K	540
0	0	Cu	1360 ± 5 K	785 ± 5 K	575
0.00115607	1	Cu+1	1340 ± 5 K	820 ± 5 K	520
0.00230947	2	Cu+2	1330 ± 5 K	765 ± 5 K	575
0.00460829	4	Cu+4	1300 ± 5 K	785 ± 5 K	515
0.00917431	8	Cu+8	1260 ± 5 K		

In the Table 3, T_m is the melting temperature and T_f is the freezing temperature. They are obtained as the averages of the range in which the phase transformations take place. The first column indicates number of defects, negative values indicating the number of vacancies and the positive values indicating the number of interstitials. In our calculations the difference between the melting and freezing temperatures obtained for pure Cu is 575K compared to 421K of X. J. Han et al. [136].

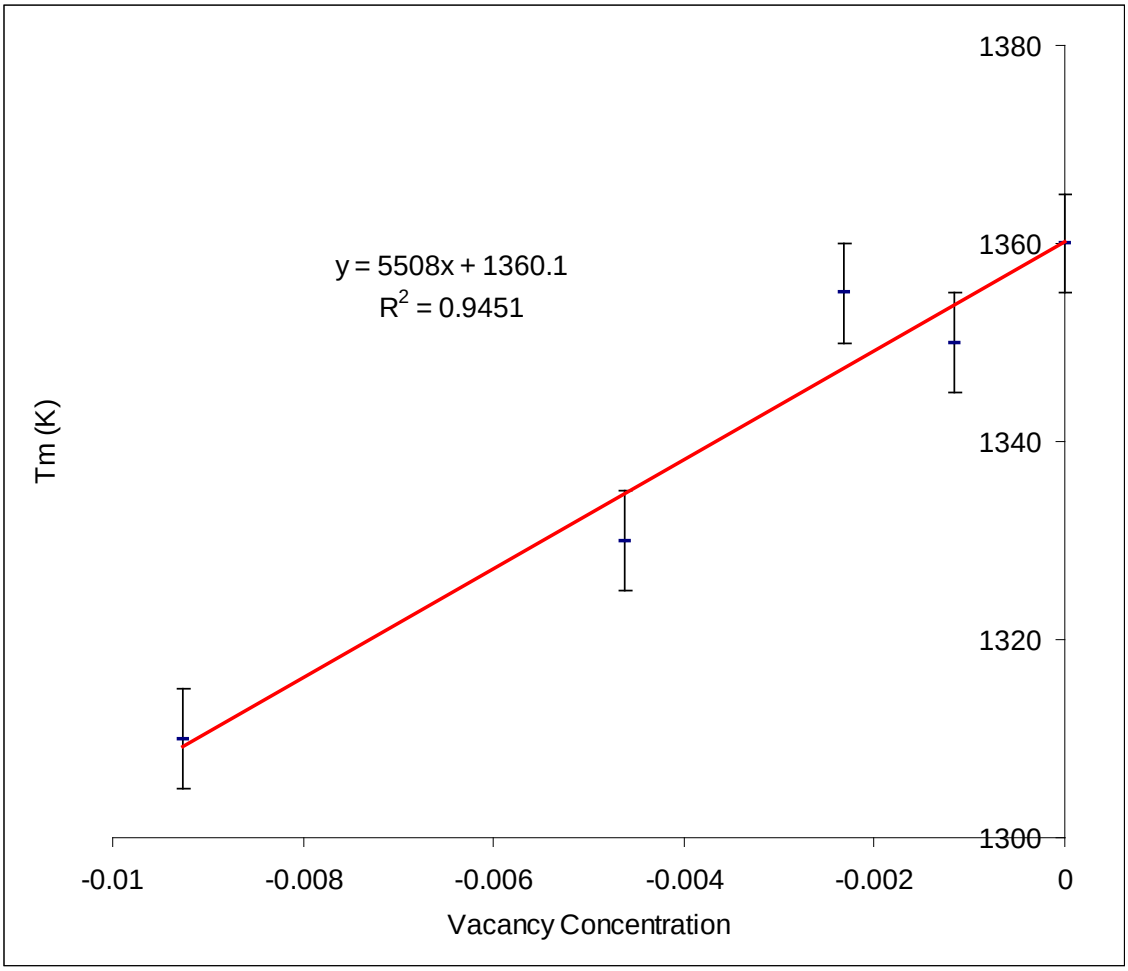

Figure 29: Melting point Vs number of vacancies

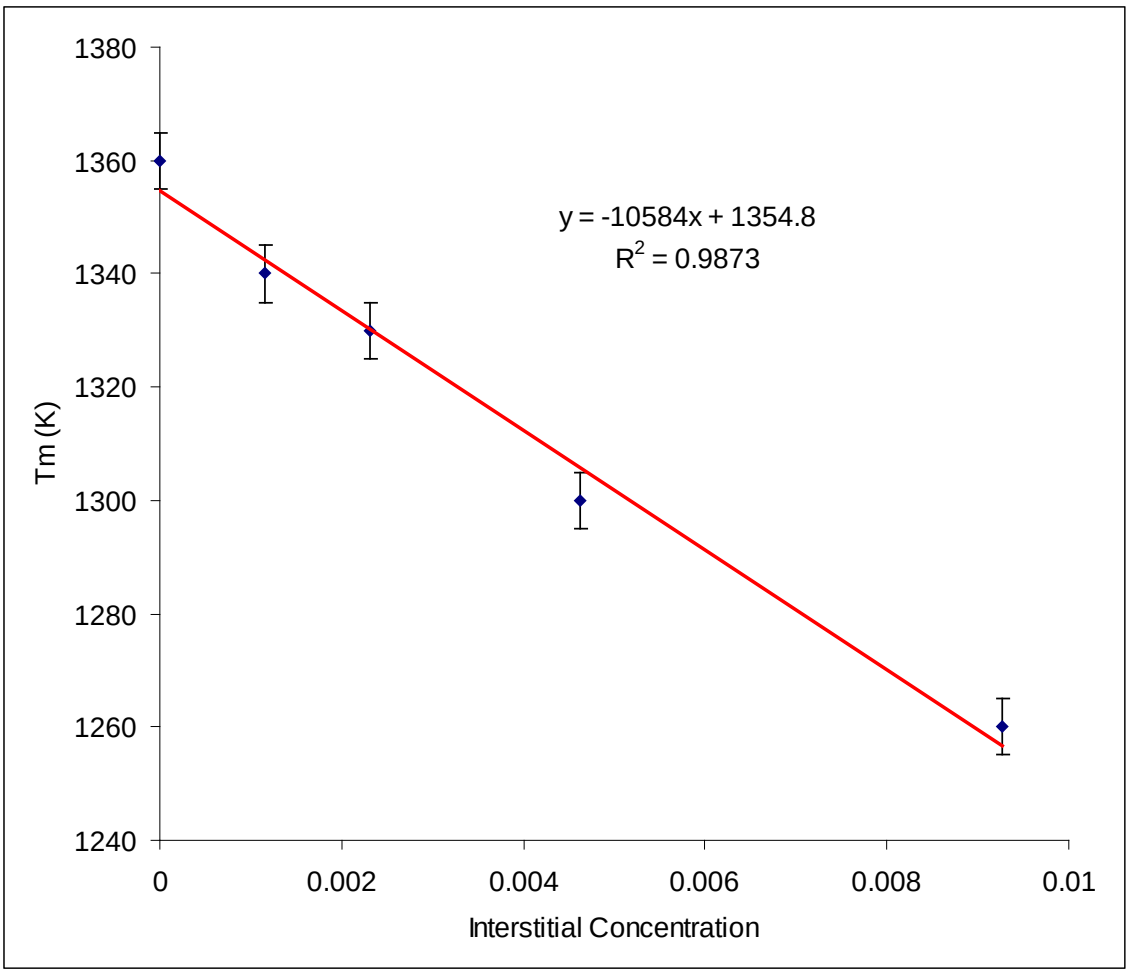

Figure 30: Melting point Vs number of interstitials

As can be seen from figure 29 and figure 30, in both vacancies as well as interstitials, melting point seems to follow a linear behavior along with the concentration of these defects. Also, for around 0.93% vacancies the T_m decreases by 3.67%, whereas for the same amount of interstitials T_m decreases by 7.35%. Thus, it is observed that the influence of an interstitial on melting point is twice that of a vacancy. Error bars are present because melting occurs in a range of temperature.

Edge dislocation: An edge dislocation structure is created as described earlier by deleting half a plane of atoms along [1 1 0] direction. The system of 3890 atoms is then heated employing constant stress–constant temperature (TtN) Molecular Dynamics. Figure 31 shows the structure of edge dislocation at 600K. It can be seen that the structure has not melted since the atoms are regular. Atoms near the edge dislocation are more distorted than those away from it. The system loses its mechanical stability at a temperature lower than 900K. Thus the system undergoes a phase transition from solid to liquid. This liquid structure can be seen in figure 32.

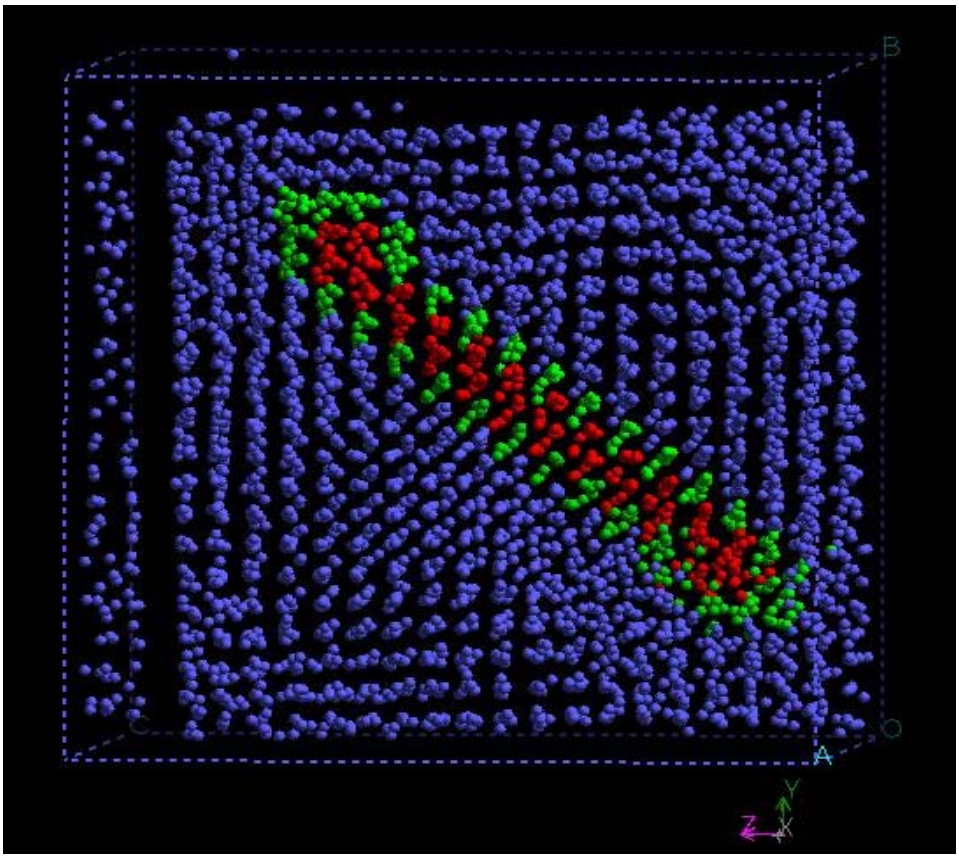

Figure 31: Edge dislocation at 600K

The red atoms are the ones that were around the deleted atoms (first nearest neighbors) and the green colored atoms are the ones surrounding the red atoms (second nearest neighbors). The edge dislocation can be considered as a very large number of vacancies as one-half plane is missing. The total number of missing atoms is 110 in this case out of 4000 atoms. Thus the edge dislocation can be imagined to be like a system with a vacancy concentration of 2.75% which is very high. This high concentration of vacancy is the reason why the system undergoes mechanical instability and hence melting.

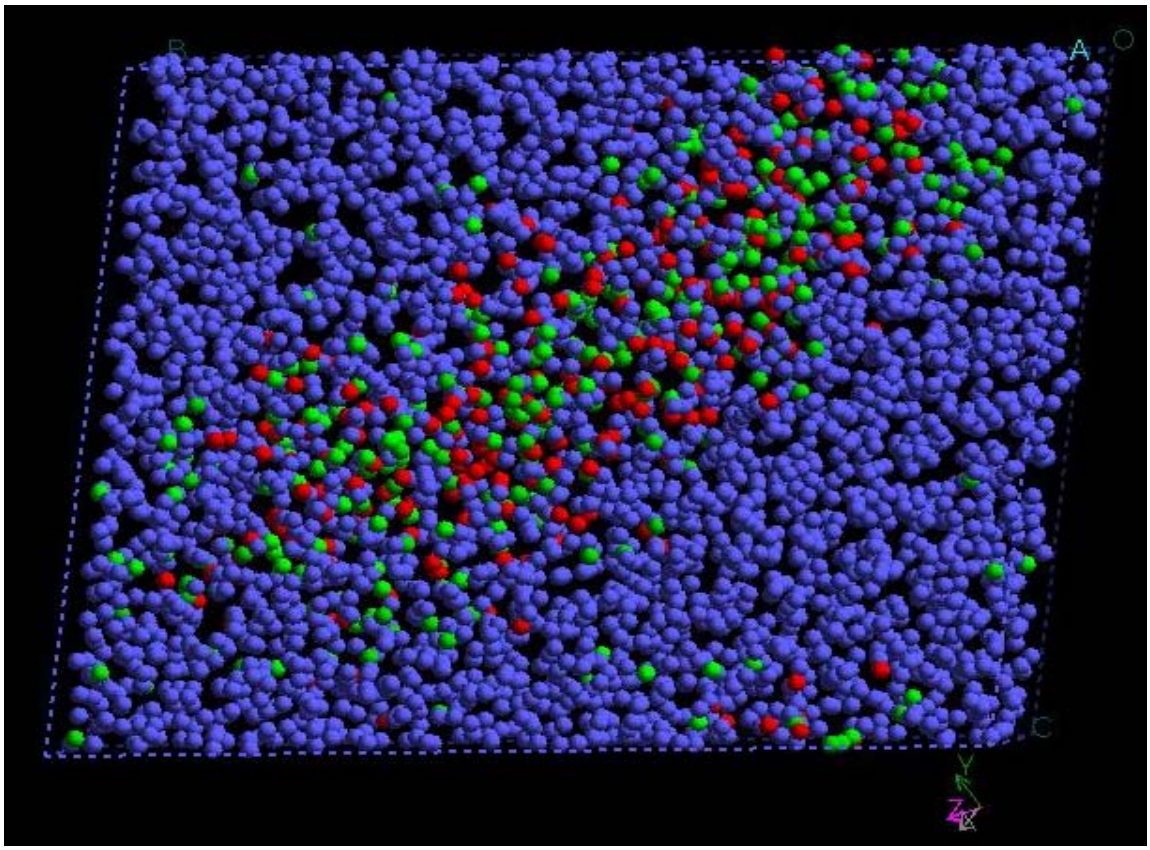

Figure 32: Edge dislocation at 900K

Grain boundary 1: A crystalline superlattice of copper with a grain boundary with 1152 atoms (Sigma3, <111>, 60.0) is formed. This is formed when the unit cell as shown in figure 33, is extended 4 times in X-direction, 3-times in Y-direction and 2+2 times in Z-direction. 2+2 signifies that the grain boundary is in Z-direction half way through the lattice and parallel to XY-plane. This grain boundary is shown in figure 8. We heat this system using TtN ensemble from 300K slowly until it melts.

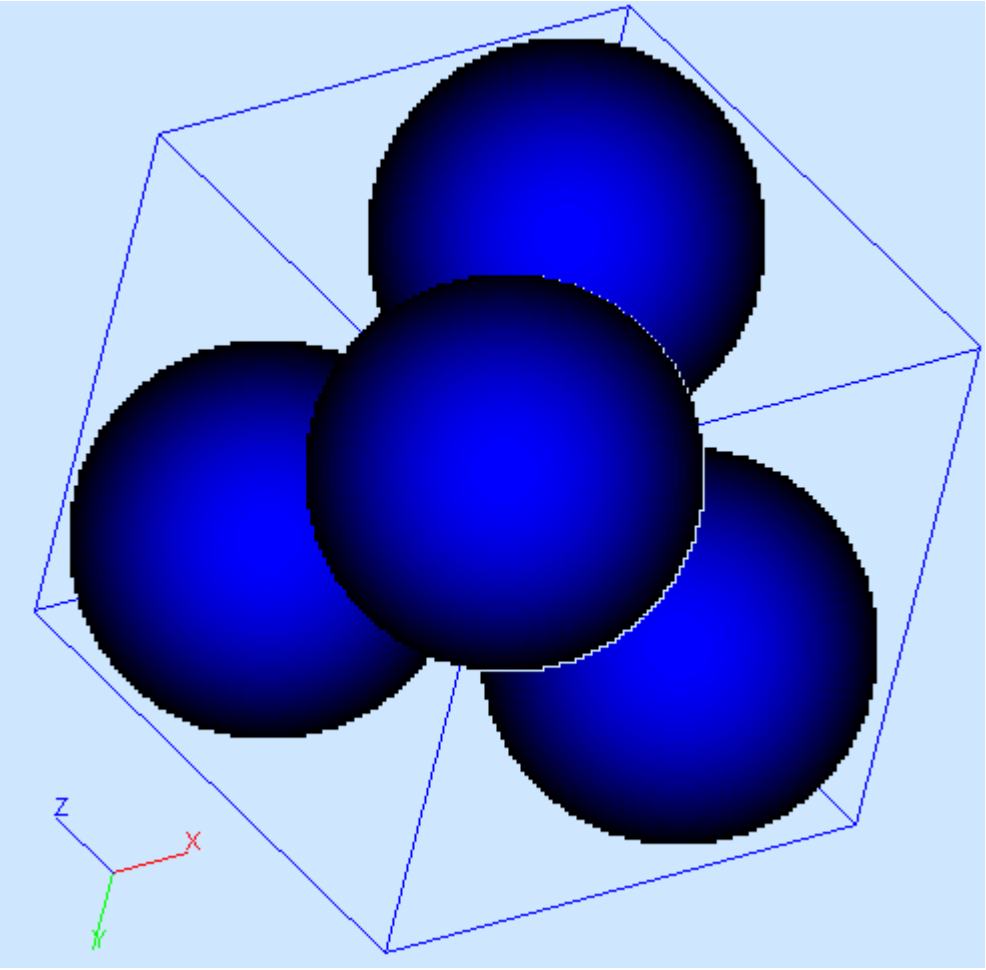

Figure 33: A unit cell of grain boundary structure using GBStudio[110]

We follow the procedure to what we did earlier and narrow down the melting point range. We see that the crystal melts in the range of 1360K – 1370K. Thus its melting point is $1365 \pm 5\,\mathrm{K}$ taking it as a centre of this range. In this range of temperature there is an unusual jump in the specific heat of the system. Also from figure 34 we see that the density of the system decreases linearly until this temperature and makes a jump downwards during the transition and again continues its linearity. Thus it is known that the system has melted. This is also confirmed from graphs of average volume as shown in figure 35.

The presence of grain boundary is expected to decrease melting point of the crystal. But in this case the melting point is actually higher than the system of copper without defects ($1360 \pm 5\,\mathrm{K}$). This might be because the copper system that we considered has less number of atoms (864) compared to the grain boundary structure of copper (1152 atoms). To verify this, we construct another structure of copper without defects consisting of 1152 atoms by taking a 6 X 6 X 8 crystalline superlattice. The same procedure as above is followed and the system is heated. From the graphs of density and average volume as shown in figure 36 and figure 37 we know that the crystal without defects melts in the range of 1365K – 1375K. Thus the melting point of this system is $1370 \pm 5\,\mathrm{K}$. This is a little higher than the melting point of the grain boundary structure which is $1365 \pm 5\,\mathrm{K}$. The melting behavior can also be seen from the radial distribution function for grain boundary structure 1 as shown in figure 38 for temperatures 1000K, 1350K and 1370K.

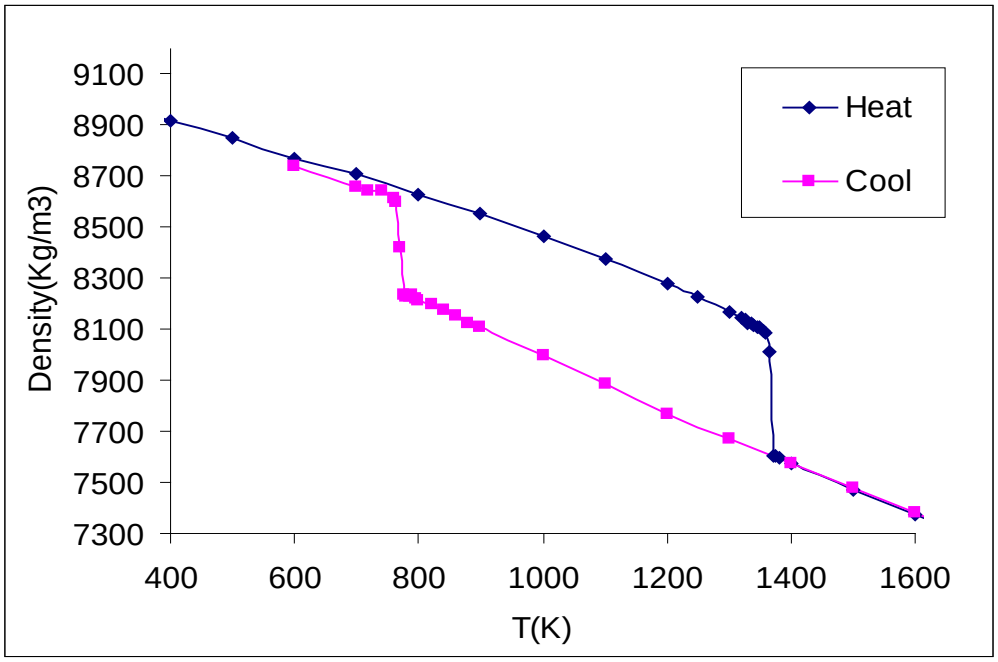

Figure 34: Density Vs temperature for grain boundary structure 1

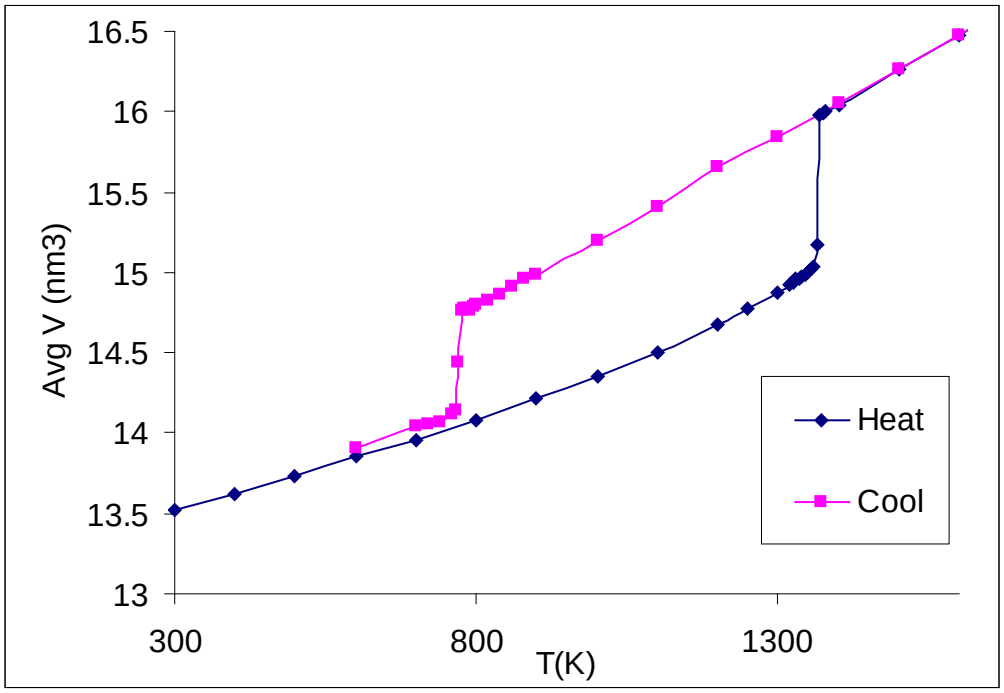

Figure 35: Average volume Vs temperature for grain boundary structure 1

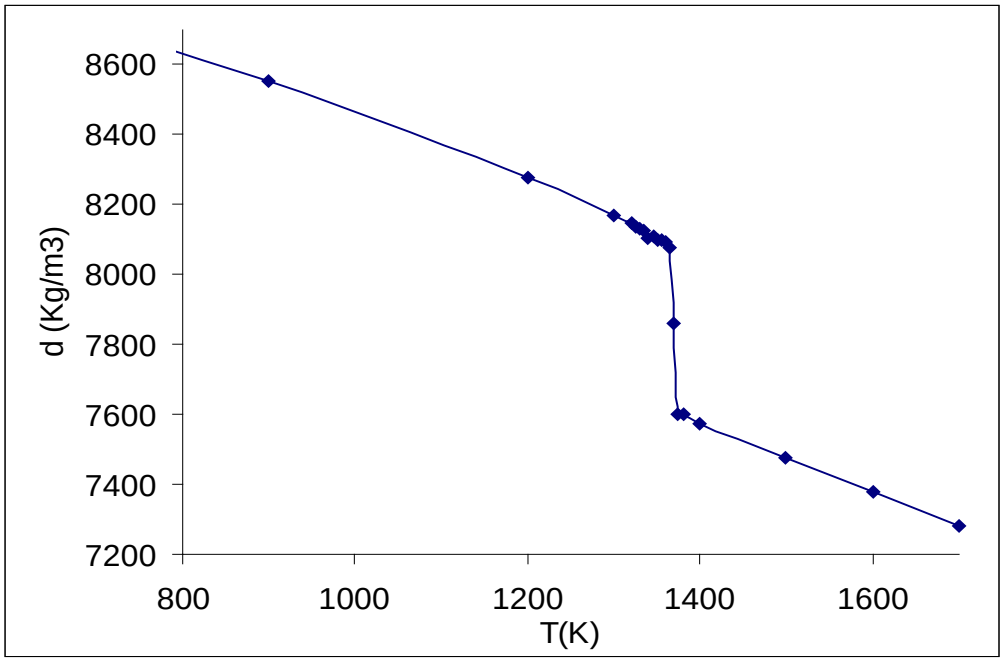

Figure 36: Density Vs temperature for copper (6X6X8 lattice) without defects

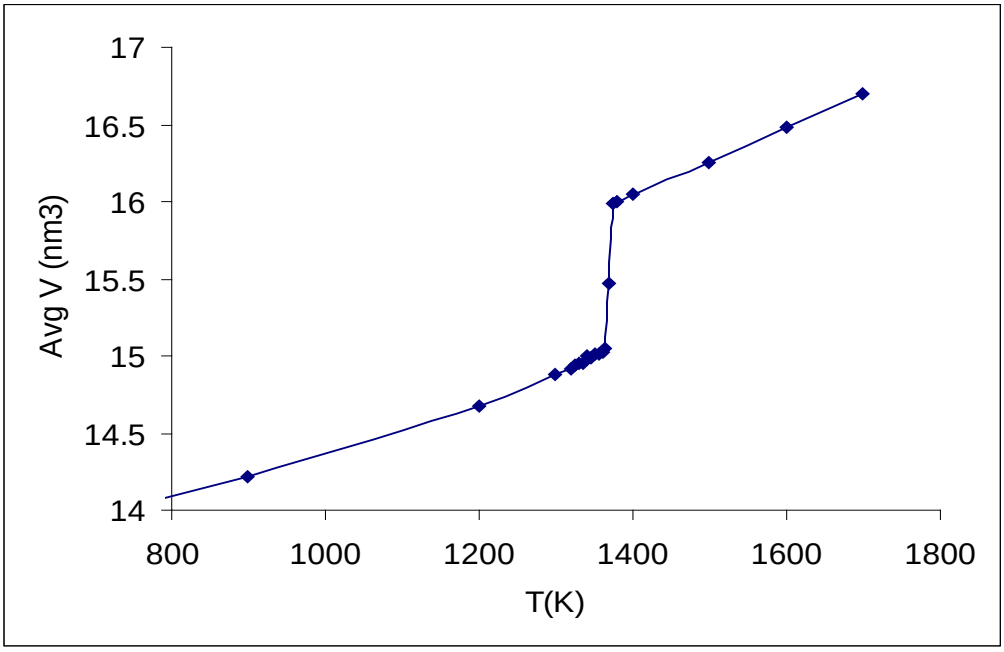

Figure 37: Average volume Vs temperature for copper (6X6X8 lattice) without defects

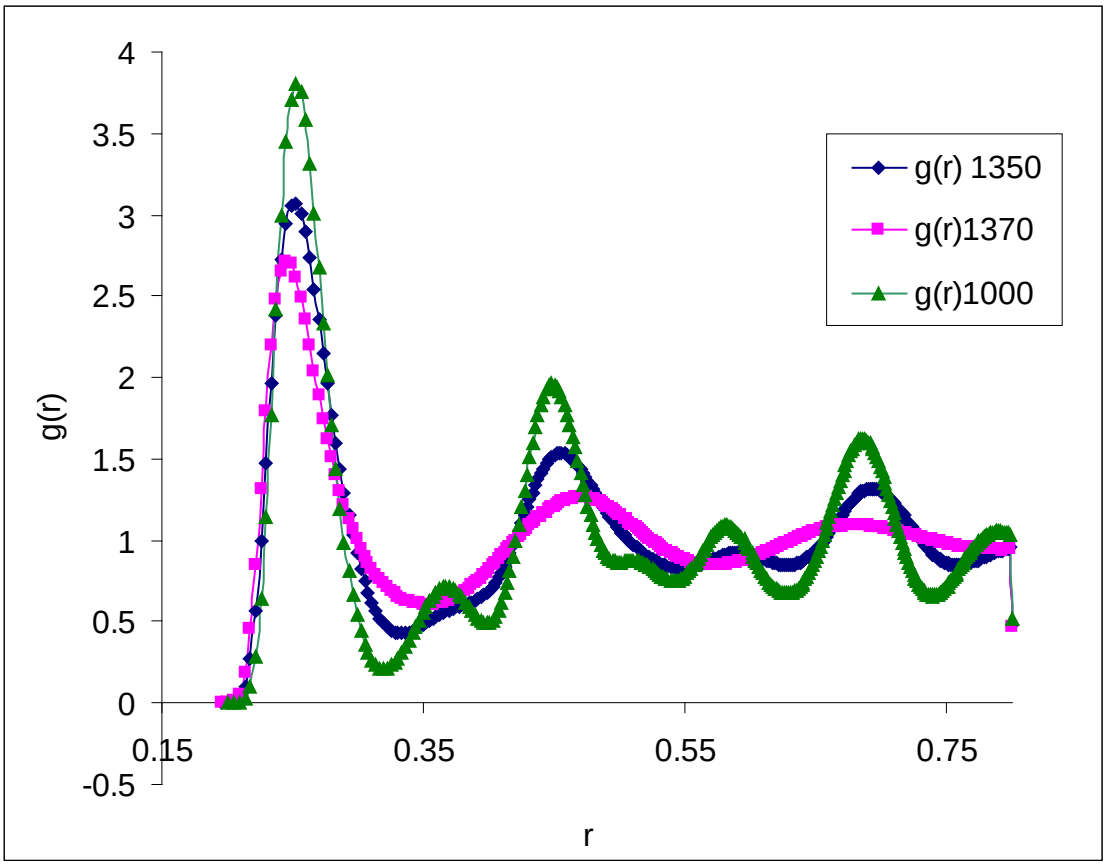

Figure 38: Radial distribution function at 1000K, 1350K and 1370K for grain boundary 1

Grain boundary 2: Another system of grain boundary is constructed which has the structure of Sigma5 <2 1 0>, 180^0. The supercell is obtained by extending the unit cell 4 times in x direction, 3 times in y direction and (2+2) times in z direction. This makes a total of 960 atoms. The grain boundary system is shown in the figure 9. This type of grain boundary system is highly mismatched at the boundary. Similar heating procedure is followed to melt the system. This system of grain boundary melts at 1275K. This is due to the type of structure of grain boundary.

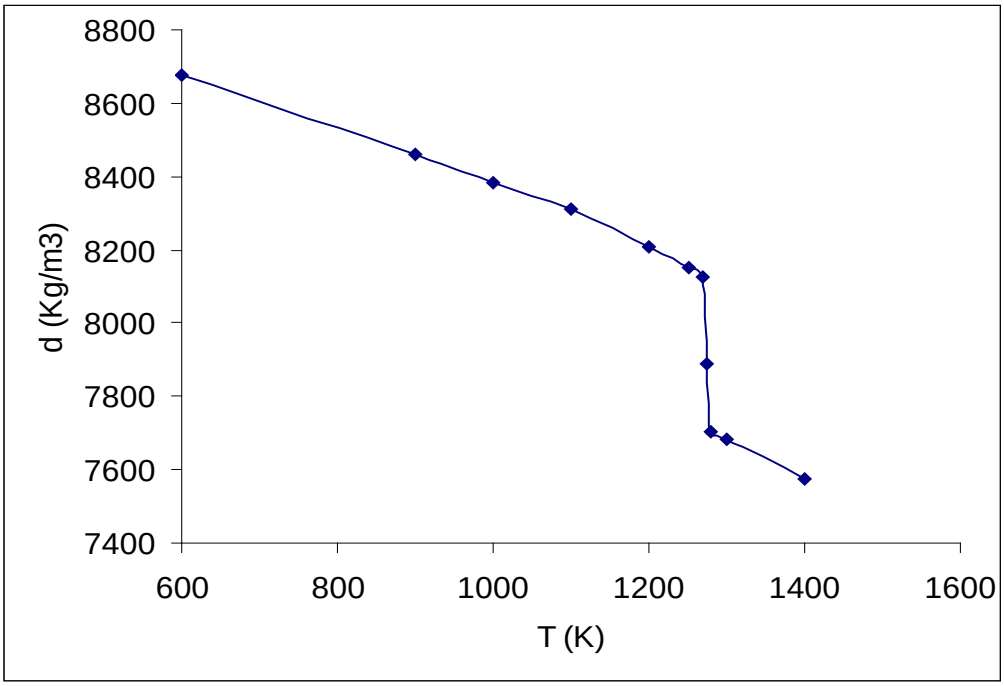

Figure 39: Density Vs temperature for copper grain boundary 2

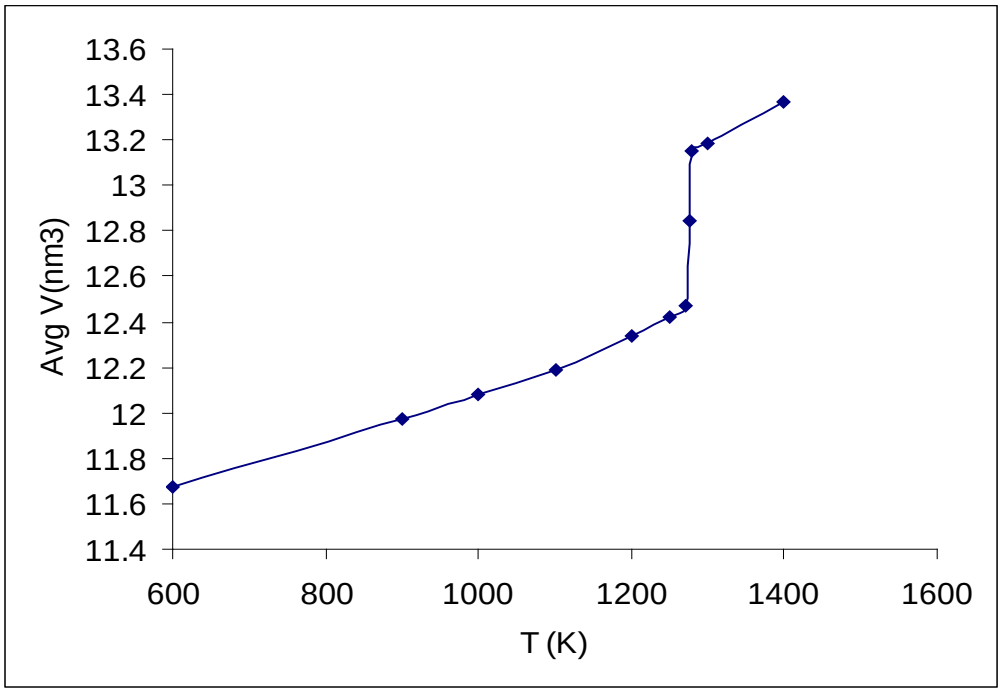

Figure 40: Average volume Vs temperature for copper grain boundary 2

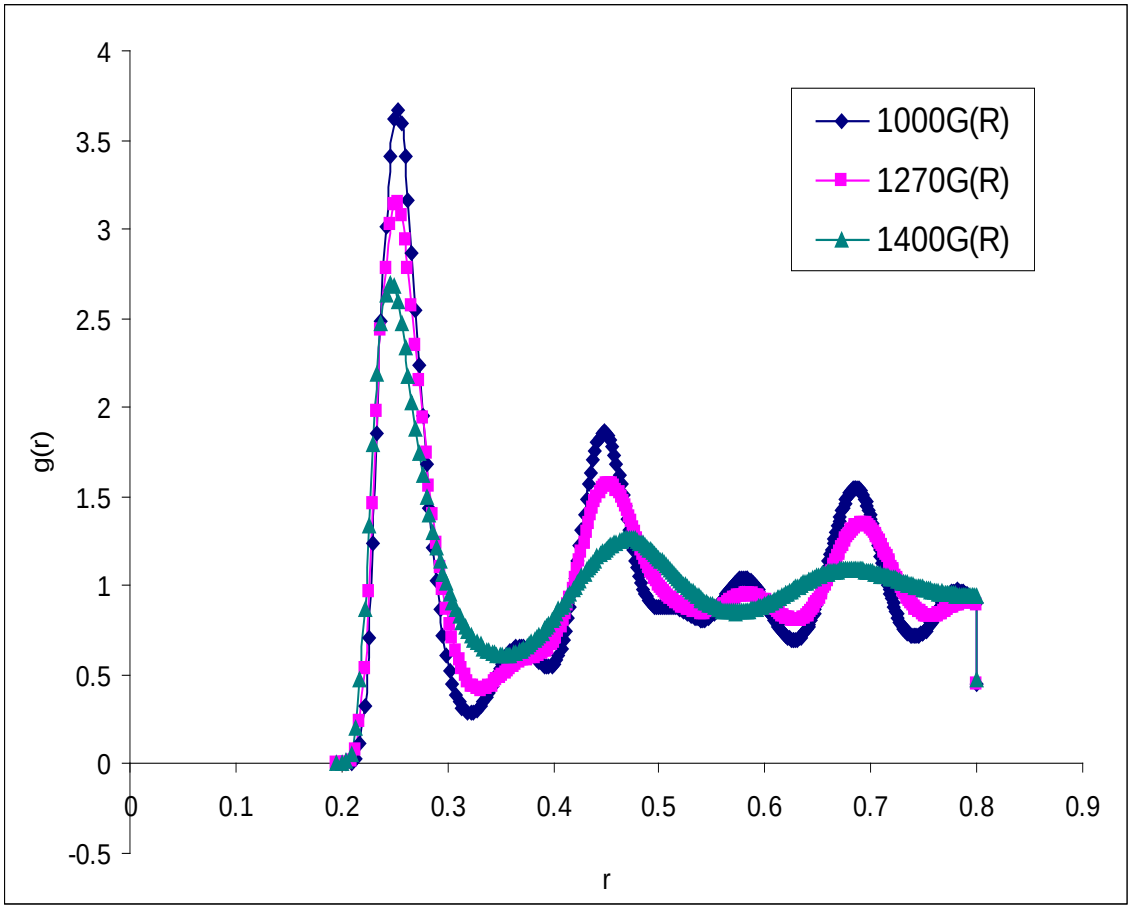

Figure 41: Radial distribution function at 1000K, 1270K and 1400K for grain boundary 2

Figure 39 and figure 40 shows how the density and average volume vary with temperature respectively. Figure 41 shows the radial distribution function for the grain boundary structure 2 at temperatures of 1000K, 1270K and 1400K. It can be seen that the first peak is high at 1000K but near the melting point it decreases. Also when the crystal melts at 1270K, the second peak almost disappears. This is another way to find out if the crystal has melted or not.

Phase coexistence simulations

Solid-liquid interface calculations are performed at various temperatures to find the true melting point of copper. For this solid and liquid structures are constructed separately. These two structures have to be at the same temperature and zero pressure. Also the interface of solid and liquid should match. These two structures are brought together and then the system is maintained at that temperature. If the solid spreads into the liquid system and there seems to be some ordering forming then it means that this temperature is below the melting temperature. Hence this procedure is repeated at a higher temperature. If the solid starts melting that means this temperature is higher than the true melting point and the next simulation is performed for a lower temperature. By this procedure one can find the true melting point of the system. As described earlier phase-coexistence structures are made for different temperatures. Here first structures are made for temperatures 900K, 950L, 1000K, 1100K, 1200K and 1300K.

First 900K structure is selected as shown in figure 42 and simulations are done for at least 20ps. After 20ps it is seen that the liquid structure on the right half of the box start to arrange themselves in an orderly manner forming layers. This can be seen in figure 43. Although this is still not completely solidified, the aim here was to see the tendency of the structure to move towards the solid or the liquid phase. In this case it goes towards a solid structure. Hence 900K is below the true melting temperature. Same procedure is now repeated taking a structure at 950K. The structure of 950K simulation after 10ps and 30ps is shown in figure 44 and figure 45 respectively.

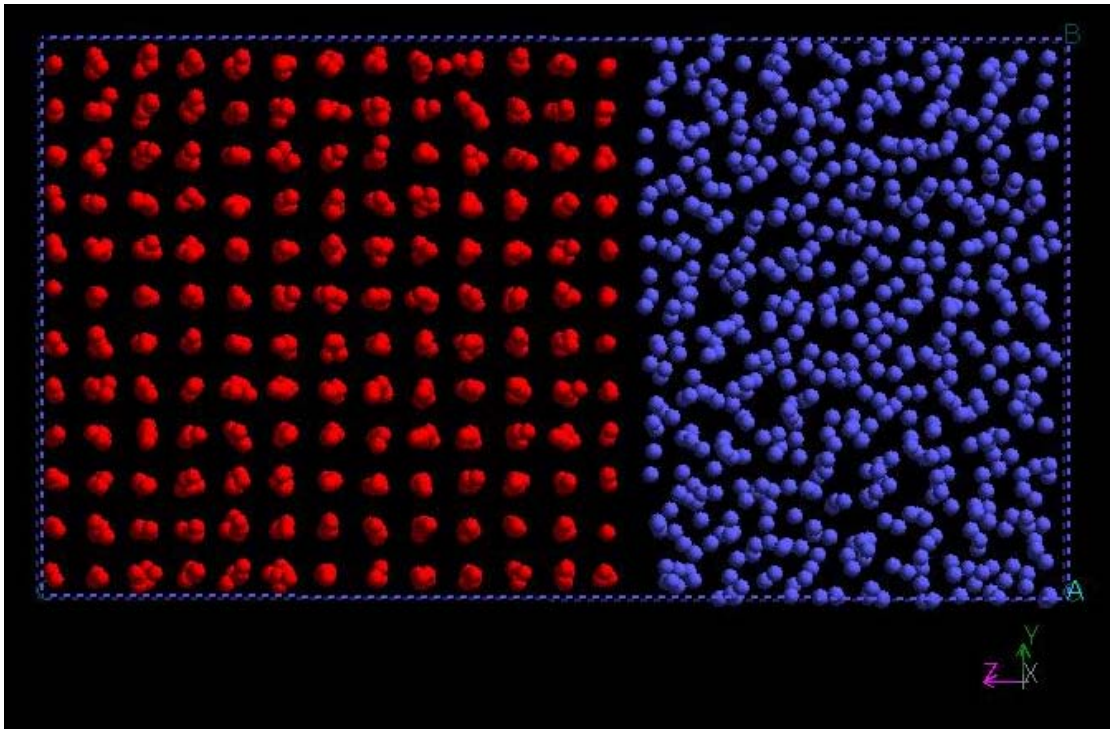

Figure 42: Phase coexistence simulation of copper at 900K at 0 ps (starting structure)

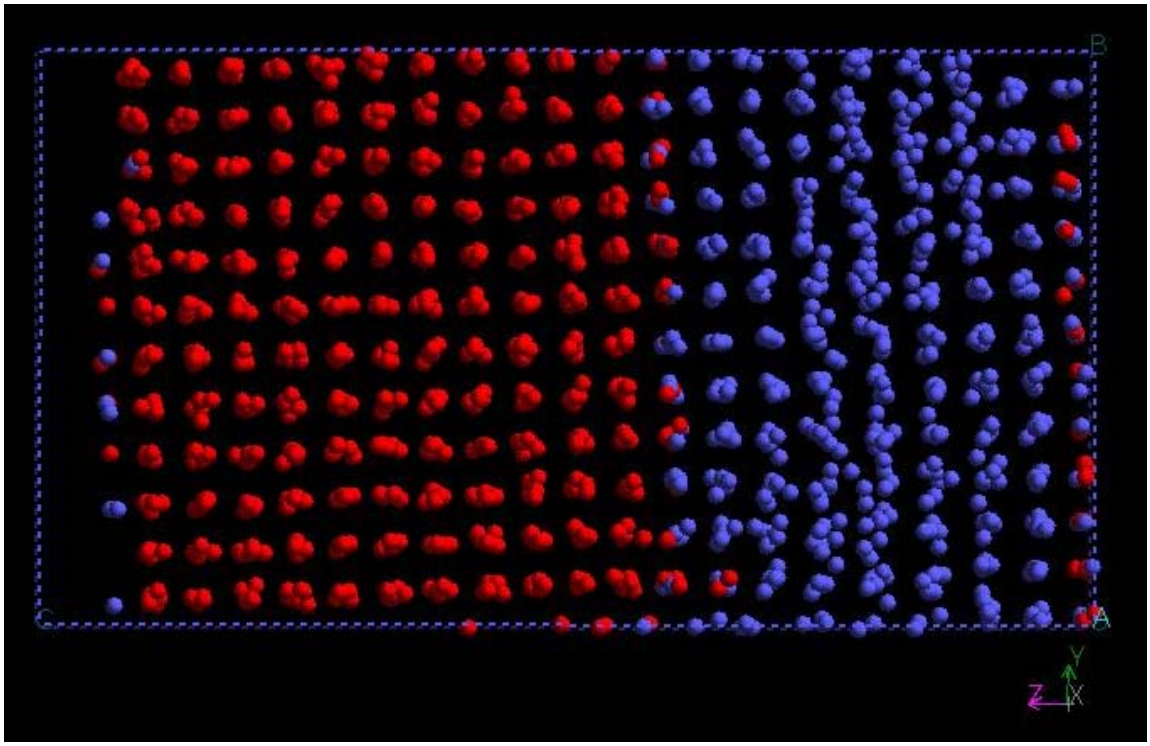

Figure 43: Phase coexistence simulation of copper at 900K at 20 ps

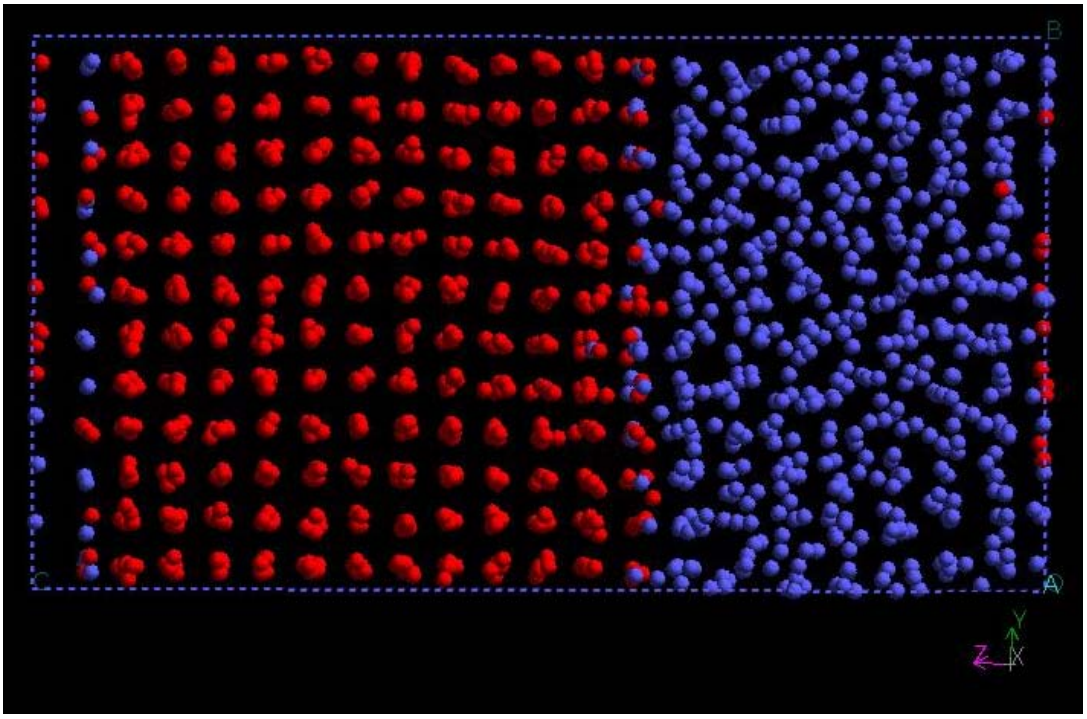

Figure 44: Phase coexistence simulation of copper at 950K after 10ps

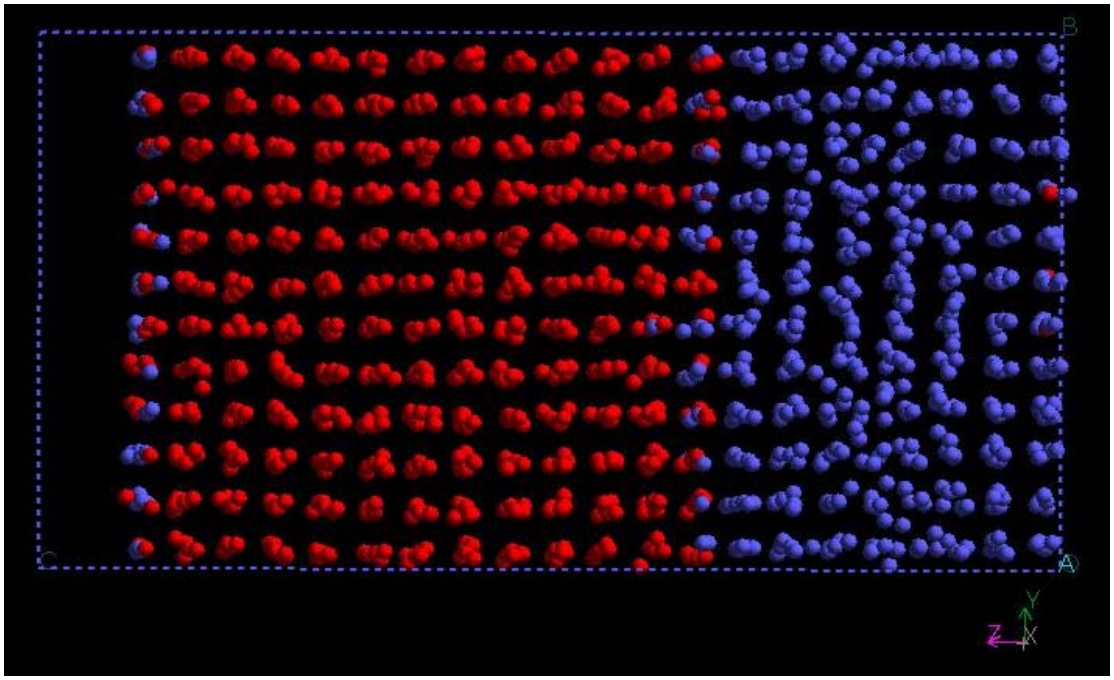

Figure 45: Phase coexistence simulation of copper at 950K after 30ps

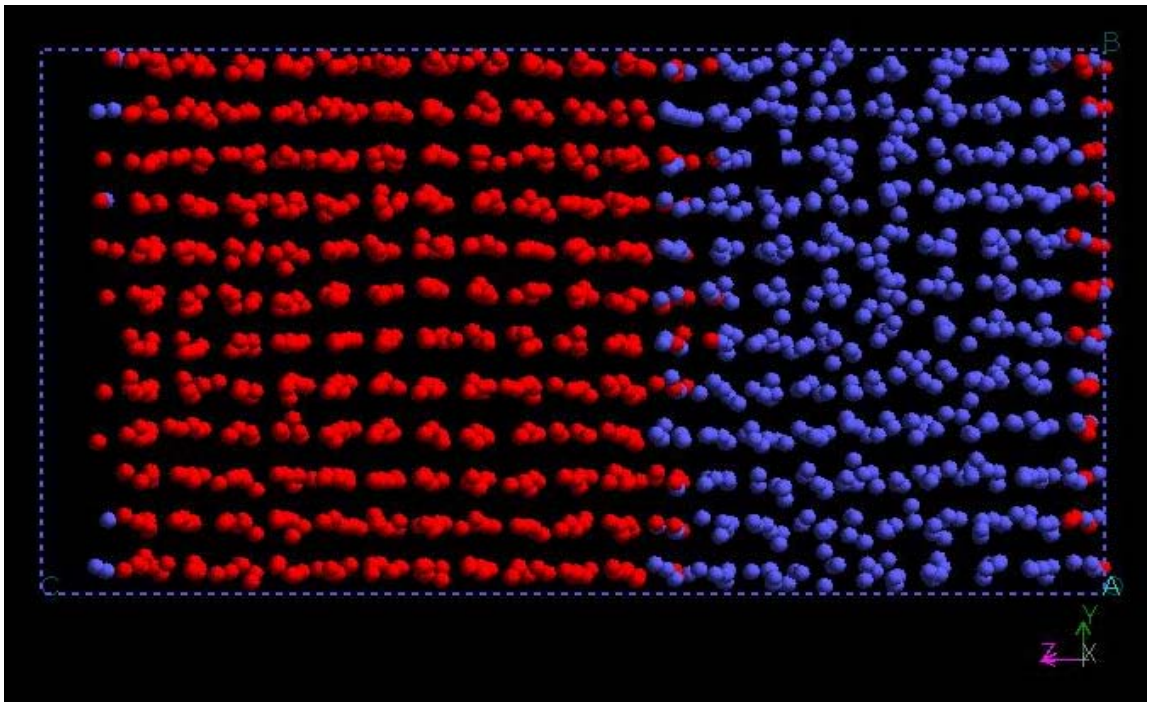

Figure 46: Phase coexistence simulation of copper at 1000K after 20ps

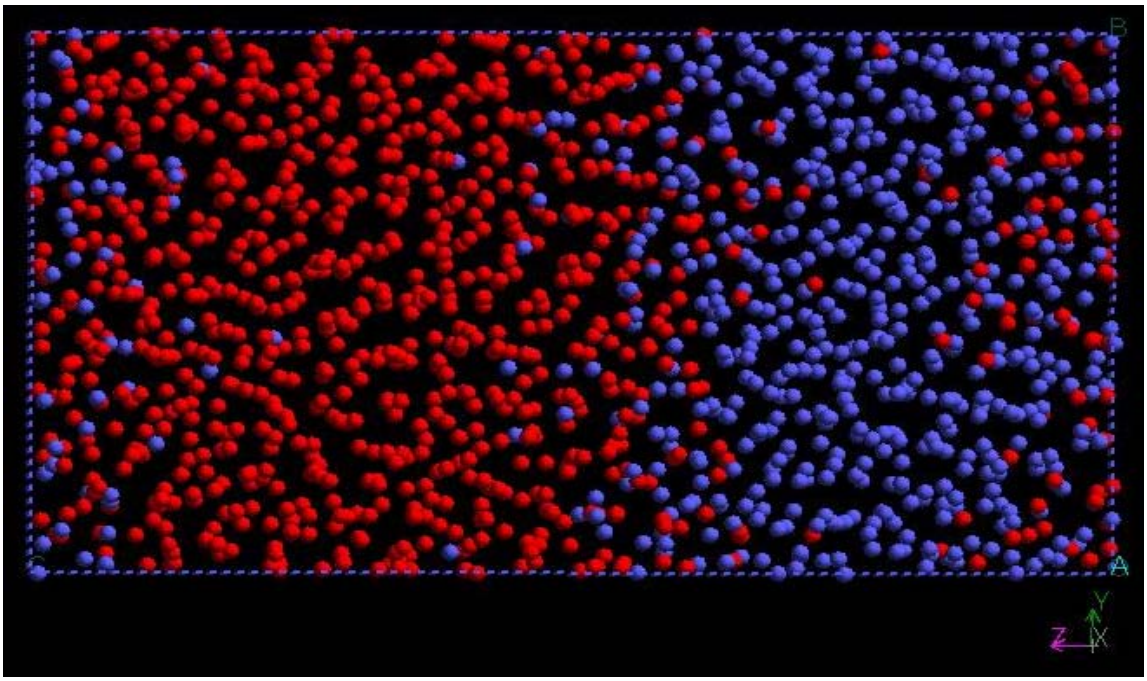

Figure 47: Phase coexistence simulation of copper at 1100K after 10ps

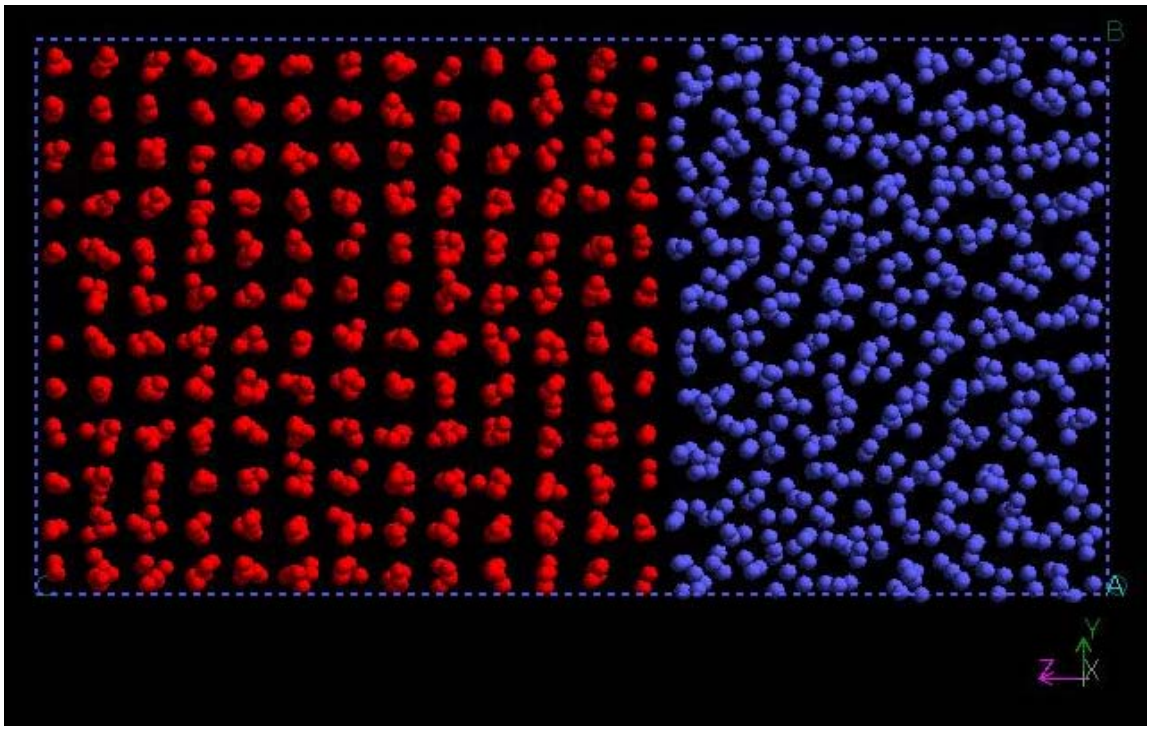

Figure 48: Phase coexistence simulation of copper at 1050K at 0ps (starting structure)

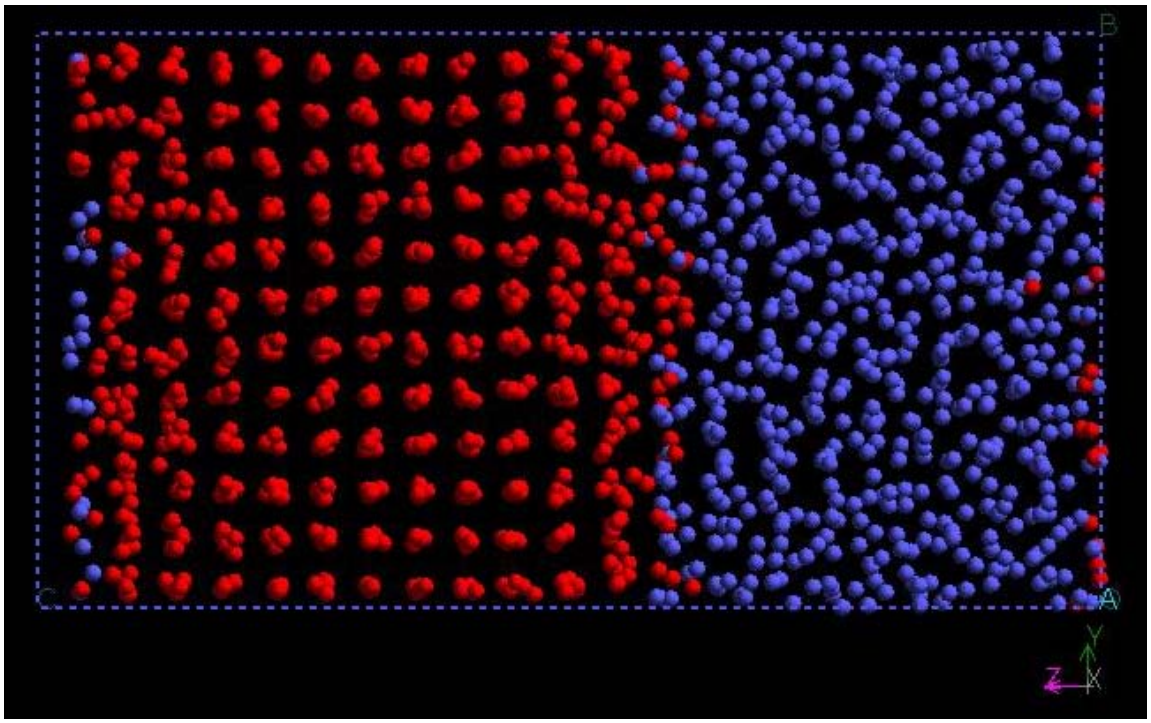

Figure 49: Phase coexistence simulation of copper at 1050K after 5ps

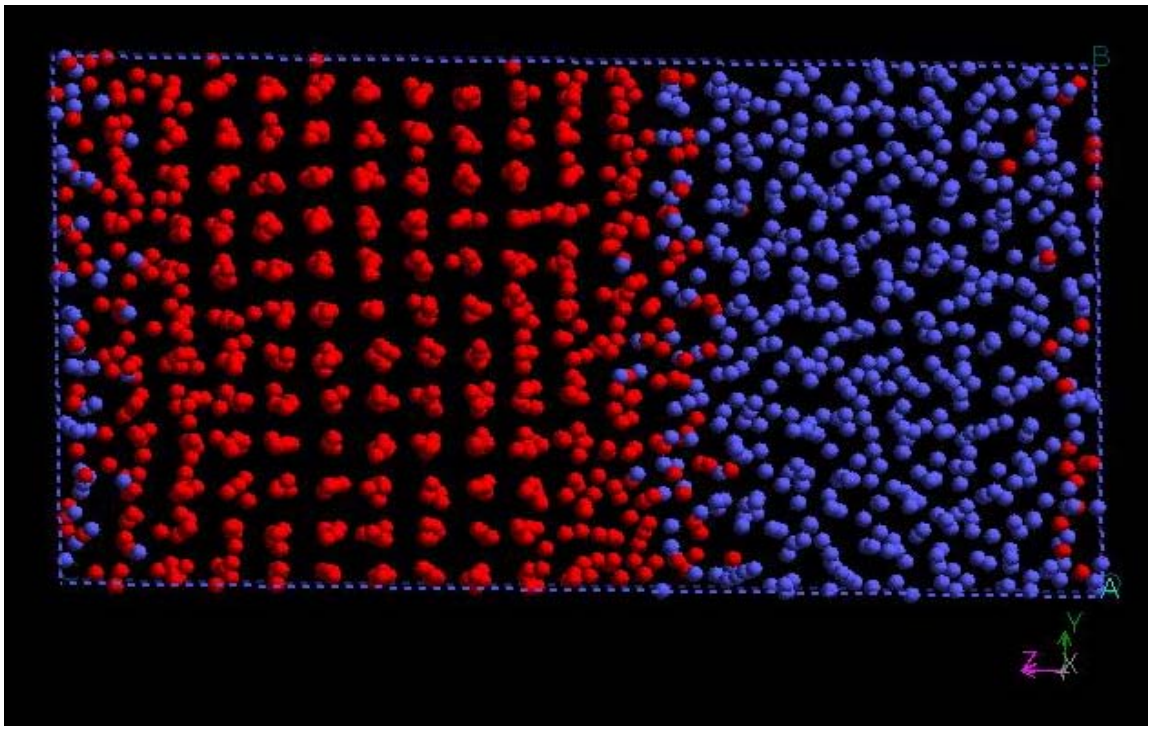

Figure 50: Phase coexistence simulation of copper at 1050K after 15ps

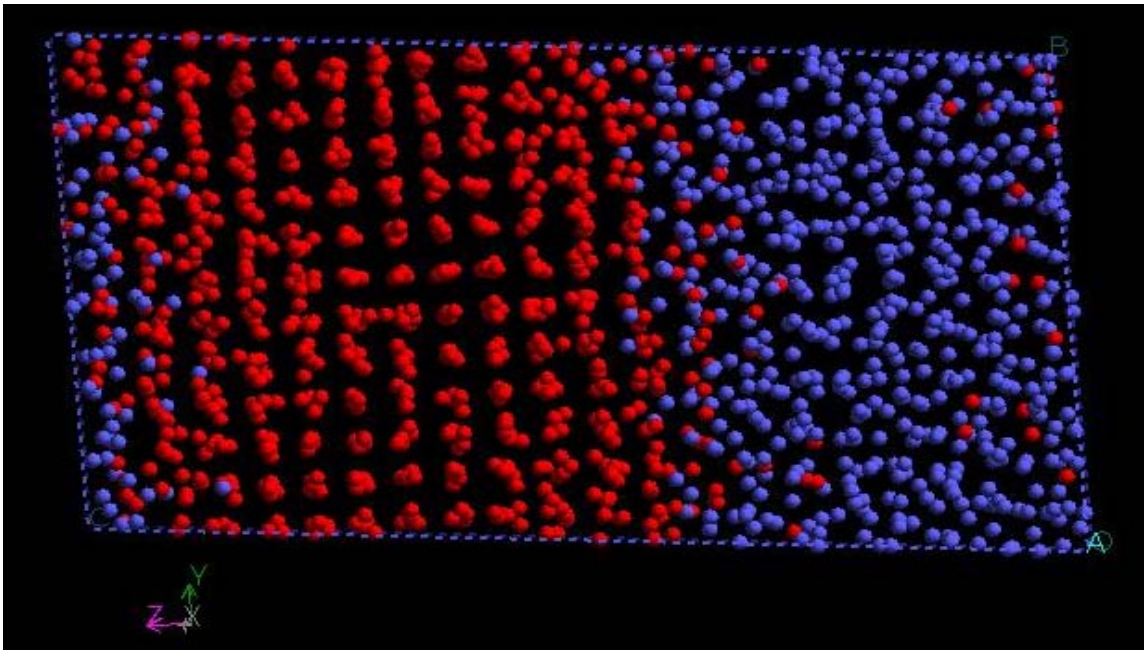

Figure 51: Phase coexistence simulation of copper at 1050K after 25ps

It can be observed that structure after 30ps is somewhat more regular than that after 10ps. Nonetheless, even the structure after 10ps is tending to order itself to form a crystal rather than melt. Thus even 950K is below the true melting point of copper. Hence the next temperature above this is selected which is 1000K. Figure 46 shows the structure that was obtained after 20ps simulations at 1000K. It is seen that again this is tending to become a solid. Therefore the next selection is done at 1100K. After about 10ps, as seen in figure 47 the atoms are disordered completely indicating the structure melts. Thus, 1100K is above the true melting temperature. Therefore the true melting temperature of copper as obtained from coexistence phase simulation is found to be between 1000K and 1100K.

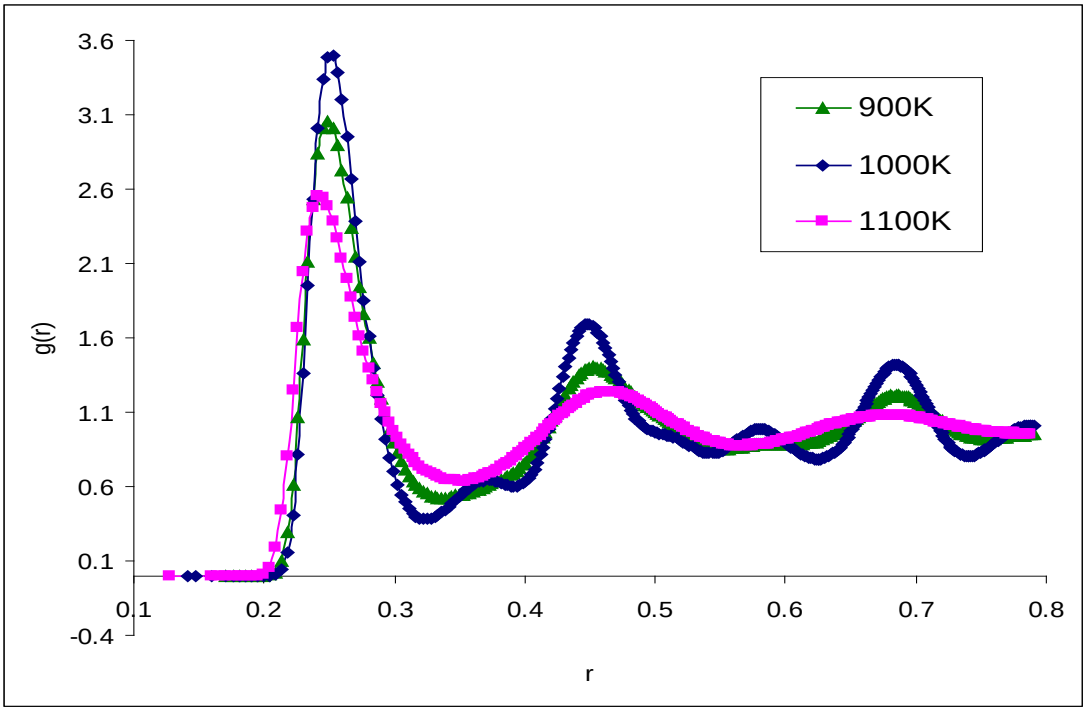

Figure 52: Radial distribution function of coexistence phase simulations at 900K, 1000K and 1100K

The next step is to choose a temperature between 1000K and 1100K. A structure is formed at 1050K for both liquid and solid and they are again brought together to perform two phase simulations. Figure 48 is the starting structure for simulations at 1050K. Figure 49, figure 50 and figure 51 are the structure after 5ps, 15ps and 25ps respectively. At 1100K the crystal had melted rapidly. This does not happen at 1050K. It can be seen that, unlike at 1100K the structure holds itself and does not melt. Thus it is safe to say that 1050K is not above the true melting temperature of copper. Also the tendency of the structure to crystallize is not really seen. The solid structure is more or less like solid and the liquid structure is like liquid. Some solid and liquid atoms have diffused into the other structure and there are some distortions at the interface which is expected anyway because of interface melting. Thus the true melting temperature of copper is $1050 \pm 25\,\mathrm{K}$.

The amount of superheating is 305K since the melting point from single phase simulation was found to be 1355K. Also the amount of supercooling is 265K as the temperature at which copper crystallizes in single phase simulations is 785K. Single phase simulations were done by applying three dimensional periodic boundary conditions which treats the crystal as a bulk and removes surface effect. This was the reason that the crystal had melted at a higher temperature and not at its true melting temperature. The radial distribution curve for these temperatures is shown in figure 52.

Vacancy clustering

Vacancy formation energy is calculated using the relation given in Ref[95]:

$$E_v^f(N) = E(N-1,1,\overline{\Omega}) - \frac{N-1}{N}E(N,0,\Omega)$$

where $E(N,v,\Omega)$ is total energy of a supercell with N atoms, v vacancies and Ω volume. There is an assumption that introduction of a vacancy does not alter the lattice constant. Vacancy formation energies calculated using various molecular dynamics methods and also by ab-intio methods are shown in Table 4. The vacancy energy calculated in this work is 1.51 eV which is very close to the experimental values.

Table 4: Vacancy formation energies for a single vacancy for copper

Method	E^f_v (eV)	
QSC MD	1.51	This work
FP-LMTO	1.33	Ref [95]
FP-LMTO	1.29	Ref [94]
LSGF ASA+M	1.33	Ref [75]
FP-KKR-GF	1.41	Ref [93, 96]
Experiment	1.28	Ref [78]
	1.28	Ref [97]
	1.19	Ref [137]

The binding energy for a divacancy can be written as

$$E_{2v}^{bind}(N;a_1,a_2) = E_{2v}^f(N;a_1,a_2) - 2E_v^f(N)$$

$E_{2v}^f(N;a_1,a_2)$ is the vacancy formation energy of a divacancy where a_1 and a_2 represent the position of the vacancies. Various binding energies calculated experimentally and computationally are shown in Table 5.

Table 5: Binding energies of divacancies in eV

	1NN E_{2v}^{bind}	E_{2v}^{bind}	
This work		-0.0548	
LSGF ASA+M	-0.096		Ref [75]
FP-KKR-GF	-0.076		Ref [138]
Divacancy on <110>	-0.19 0.05		Ref [139] Ref [71]
Divacancy on <100>	-0.23 -0.04		Ref [139] Ref [71]
Experimental	-0.2 -0.3		Ref [78] Ref [73]

Binding energy is found to be -0.0548 eV when the two vacancies are kept farther apart when calculated from Molecular Dynamics using QSC potentials. This shows that even when vacancies are kept at a distance, they tend to attract each other.

CHAPTER V

CONCLUSION

The crystallization/freezing and melting phenomena are critical in processing of chemicals and materials. In this work we studied the melting and freezing process for a model system of copper with and without defects. We studied point defects (1, 2, 4, 8 vacancies and 1, 2, 4, 8 interstitials), line defects (edge dislocation) and surface defects (grain boundary) using Molecular Dynamics simulations. Constant stress-constant temperature ensemble with atmospheric pressures is employed. The properties like average volume, potential energy, total energy, and density vary linearly before and after the phase transitions. During the transition process they show a dramatic change. This change is a sign of transition. The heat capacity also makes a jump at the phase transition giving an indication of the same. In both cases of vacancies and interstitials a decrease in the melting point is seen along with the increase in concentration. Also the melting point is seen to be following a linear behavior with the number of defects. Another observation is that the effect of presence of an interstitial on the melting point is nearly double than that of a vacancy. This is reiterating the fact that interstitials have more effect on mechanical instability. For copper with no defects the melting point is found to be $1360 \pm 5\,\mathrm{K}$. This is the upper limit to the phase transition temperature. This is because it has been obtained for a system representing a bulk crystal and having no surface effect. Also on cooling the crystal, the phase transition from liquid to solid occurs at $785 \pm 5\,\mathrm{K}$.

This is the lower limit to the phase transition temperature. The true melting point of copper will be between these two temperatures.

To overcome this hysteresis effect and obtain the true melting point, two phase calculation of copper system with no defects are performed. Using this method the true melting point of copper with no defects was found to be 1050 ± 25 K. This temperature falls in between the phase transition temperatures obtained from single phase simulations. This is because of the application of periodic boundary condition and lack of a surface in single phase simulations. Thus the amount of superheating obtained is 305K and the amount of supercooling obtained is 265K.

The influence of other type of defects such as edge dislocation and grain boundaries is also studied. The structure having an edge dislocation on [1 1 0] plane melts at a temperature lower than 900K. This is due to the absence of atoms of half a plane along that direction. An edge dislocation can be imagined as a large number of vacancies, in this case 2.75 %. Thus with such large number of vacancies there is a drastic decrease in the melting point.

Two grain boundary systems are selected for the calculations. The first system which is Sigma 3, <111>, 60^0 represents less mismatch at the grain boundary and the second system which is Sigma5, <2 1 0>, 180^0 represents more mismatch at the grain boundary. From the grain boundary calculations it is seen that, the less mismatched grain boundary does not have a large effect on the melting point, whereas the more mismatched grain boundary decreases the melting point drastically. The second grain boundary structure is not far from mechanical instability hence melts faster.

The vacancy formation energy of a single vacancy is found to be 1.51 eV at ambient conditions which is very close to the experimental values. The binding energy of a system with two vacancies is obtained to be -0.0548 eV which is negative, suggesting that the vacancies in this case attract each other. Thus it is shown that when two vacancies are present in a crystal, they tend to come together to cluster and form a larger cavity in the system. Most of the literature dealing with melting/crystallization on the basis of atomistic simulation does not include the influence of the presence of defects. Thus this work has a bearing on the various theories of melting.

REFERENCES

(1) Lawson, A. C. *Phil. Mag.* **2001**, B, 255.

(2) Ubbelohde, A. R. *The Molten State of Matter*; John Wiley & Sons: Chichester, West Sussex, UK, **1978**.

(3) Löwen, H.; Palberg, T.; Simon, R. *Physical Review Letters* **1993**, 70, 1557.

(4) Meijer, E. J.; Frenkel, D. *The Journal of Chemical Physics* **1991**, 94, 2269.

(5) Cho, S. A. *Journal of Physics F: Metal Physics* **1982**, 12, 1069.

(6) Gilvarry, J. J. *Physical Review* **1956**, 102, 308.

(7) Hansen, J.-P.; Verlet, L. *Physical Review* **1969**, 184, 151.

(8) Martin, C. J.; O'Connor, D. A. *Journal of Physics C: Solid State Physics* **1977**, 10, 3521.

(9) Ross, M. *Physical Review* **1969**, 184, 233.

(10) Shapiro, J. N. *Physical Review B* **1970**, 1, 3982.

(11) Stern, E. A.; Zhang, K. *Physical Review Letters* **1988**, 60, 1872.

(12) Stillinger, F. H.; Weber, T. A. *Physical Review B* **1980**, 22, 3790.

(13) Wolf, G. H.; Jeanloz, R. *Journal of Geophysical Research* **1984**, 89, 7821.

(14) Young, D. A.; Alder, B. J. *The Journal of Chemical Physics* **1974**, 60, 1254.

(15) Hoover, W. G.; Gray, S. G.; Johnson, K. W. *The Journal of Chemical Physics* **1971**, 55, 1128.

(16) Jin, Z. H.; Gumbsch, P.; Lu, K.; Ma, E. *Physical Review Letters* **2001**, 8705.

(17) Luo, S. N.; Strachan, A.; Swift, D. C. *Journal of Chemical Physics* **2004**, 120, 11640.

(18) Poirier, J. P. *Introduction to the Physics of the Earth's Interior* Cambridge University Press: New York, **1991**.

(19) Born, M. *Journal of Chemical Physics* **1939**, 7, 591.

(20) Kanigel, A.; Adler, J.; Polturak, E. *International Journal of Modern Physics C* **2001**, 12, 727.

(21) Granato, A. *Metallurgical and Materials Transactions A* **1998**, 29, 1837.

(22) Broughton, J. Q.; Gilmer, G. H.; Weeks, J. D. *Physical Review B* **1982**, 25, 4651.

(23) Frenkel, D. *Kinetic Theory of Liquids*; Dover Publications, Inc.: New York, **1955**.

(24) Lennard-Jones, J. E.; Devonshire, A. F. *Proceedings of the Royal Society of London. Series A, Mathematical and Physical Sciences (1934-1990)* **1939**, 169, 317.

(25) Lennard-Jones, J. E.; Devonshire, A. F. *Proceedings of the Royal Society of London. Series A, Mathematical and Physical Sciences (1934-1990)* **1939**, 170, 464.

(26) Cotterill, R. M. J. *Journal of Crystal Growth* **1980**, 48, 582.

(27) Gorecki, T. *Zeitschrift fuer Metallkunde/Materials Research and Advanced Techniques* **1974**, 65, 426.

(28) Gorecki, T. *Zeitschrift fuer Metallkunde/Materials Research and Advanced Techniques* **1976**, 67, 269.

(29) Mei, Q. S.; Lu, K. *Philosophical Magazine Letters* **2008**, 88, 203.

(30) Carnevali, P.; Ercolessi, F.; Tosatti, E. *Physical Review B* **1987**, 36, 6701.

(31) Pluis, B.; van der Gon, A. W. D.; Frenken, J. W. M.; van der Veen, J. F. *Physical Review Letters* **1987**, 59, 2678.

(32) van der Gon, A. W. D.; Smith, R. J.; Gay, J. M.; O'Connor, D. J.; van der Veen, J. F. *Surface Science* **1990**, 227, 143.

(33) Sun, D. Y.; Shu, D. J.; Gong, X. G.; Lau, L. W. M. *Solid State Communications* **1998**, 108, 383.

(34) Di Tolla, F. D.; Ercolessi, F.; Tosatti, E. *Physical Review Letters* **1995**, 74, 3201.

(35) Frenken, J. W. M.; Veen, J. F. v. d. *Physical Review Letters* **1985**, 54, 134.

(36) Daeges, J.; Gleiter, H.; Perepezko, J. H. *Physics Letters* A **1986**, 119, 79.

(37) Khaikin, S. E.; Bene, N. R. C. R. *Acad. Sci*.URSS **1939**, 23.

(38) Nguyen, T.; Ho, P. S.; Kwok, T.; Nitta, C.; Yip, S. *Physical Review Letters* **1986**, 57, 1919.

(39) Ciccotti, G.; Guillopé, M.; Pontikis, V. *Physical Review B* **1983**, 27, 5576.

(40) Nguyen, T.; Ho, P. S.; Kwok, T.; Nitta, C.; Yip, S. *Physical Review B* **1992**, 46, 6050.

(41) Lutsko, J. F.; Wolf, D.; Yip, S.; Phillpot, S. R.; Nguyen, T. *Physical Review B* **1988**, 38, 11572.

(42) Broughton, J. Q.; Gilmer, G. H. *Physical Review Letters* **1986**, 56, 2692.

(43) Lutsko, J. F.; Wolf, D.; Phillpot, S. R.; Yip, S. *Physical Review B* **1989**, 40, 2841.

(44) Kikuchi, R.; Cahn, J. W. *Physical Review B* **1980**, 21, 1893.

(45) Plimpton, S. J.; Wolf, E. D. *Physical Review B* **1990**, 41, 2712.

(46) Carrion, F.; Kalonji, G.; Yip, S. *Scripta Metallurgica* **1983**, 17, 915.

(47) Fan, W.; He, Y. Z.; Gong, X. G. *Philosophical Magazine a-Physics of Condensed Matter Structure Defects and Mechanical Properties* **1999**, 79, 1321.

(48) Alder, B. J.; Wainwright, T. E. *The Journal of Chemical Physics* **1959**, 31, 459.

(49) Morris, J. R.; Wang, C. Z.; Ho, K. M.; Chan, C. T. *Physical Review B* **1994**, 49, 3109.

(50) Jin, Z. H.; Lu, K. *Philosophical Magazine Letters* **1998**, 78, 29.

(51) Strachan, A.; Cagin, T.; Goddard, W. A. *Physical Review B* **1999**, 60, 15084.

(52) Luo, S. N.; Cagin, T.; Strachan, A.; Goddard, W. A.; Ahrens, T. J. *Earth and Planetary Science Letters* **2002**, 202, 147.

(53) Allen, M. P.; Tildesley, D. J. *Computer Simulation of Liquids*; Clarendon Press; Oxford University Press: Oxford England, **1987**.

(54) Smolander, K. J. *Physica Scripta* **1990**, *42*, 485.

(55) Wu, Z. M.; Wang, X. Q.; Yang, Y. Y. *Chinese Physics* **2007**, 16, 405.

(56) Mei, J.; Davenport, J. W.; Fernando, G. W. *Physical Review B* **1991**, 43, 4653.

(57) Buffat, P.; Borel, J. P. *Physical Review A* **1976**, 13, 2287.

(58) Ercolessi, F.; Andreoni, W.; Tosatti, E. *Physical Review Letters* **1991**, 66, 911.

(59) Valkealahti, S.; Manninen, M. *Zeitschrift Fur Physik D-Atoms Molecules and Clusters* **1993**, 26, 255.

(60) bvLuo, S. N.; Zheng, L. Q.; Tschauner, O. *Journal of Physics-Condensed Matter* **2006,** 18, 659.

(61) Dederichs, P. H.; Lehmann, C.; Schober, H. R.; Scholz, A.; Zeller, R. *Journal of Nuclear Materials* **1978**, 69-70, 176.

(62) Rehn, L. E.; Holder, J.; Granato, A. V.; Coltman, R. R.; Young, F. W. *Physical Review B* **1974**, 10, 349.

(63) Mehrer, H. *Journal of Nuclear Materials* **1978**, 69-70, 38.

(64) Vikram, G.; Kaushik, B.; Michael, O. Vacancy clustering and prismatic dislocation loop formation in aluminum; APS, **2007**; Vol. 76; pp 180101.

(65) Bullough, T. J.; English, C. A.; Eyre, B. L. Low-energy heavy-ion irradiations of copper and molybdenum at low temperatures; *The Royal Society,* **1991**; Vol. 435; pp 85.

(66) Eyre, B. L.; Bartlett, A. F. *Phil. Mag.* **1965**, *8*, 261.

(67) Masters, B. C. *Nature* **1963**, *200*, 254.

(68) Horton, L. L.; Farrel, K. *J. Nucl. Mater* **1984**, 684.

(69) Kawanishi, H.; Kuramoto, E. *J. Nucl. Mater* **1986**, 899.

(70) Marian, J.; Wirth, B. D.; Perlado, J. M. *Physical Review Letters* **2002**, 88, 255507.

(71) Carling, K.; Wahnström, G.; Mattsson, T. R.; Mattsson, A. E.; Sandberg, N.; Grimvall, G. *Physical Review Letters* **2000**, 85, 3862.

(72) Fluss, M. J.; Berko, S.; Chakraborty, B.; Hoffmann, K. R.; Lippel, P.; Siegel, R. W. *Journal of Physics F: Metal Physics* **1984**, 14, 2831.

(73) Hehenkamp, T. *Journal of Physics and Chemistry of Solids* **1994**, 55, 907.

(74) Uesugi, T.; Kohyama, M.; Higashi, K. *Physical Review B* **2003**, 68, 184103.

(75) Korzhavyi, P. A.; Abrikosov, I. A.; Johansson, B.; Ruban, A. V.; Skriver, H. L. *Physical Review B* **1999**, 59, 11693.

(76) Gavini, V.; Knap, J.; Bhattacharya, K.; Ortiz, M. *Journal of the Mechanics and Physics of Solids* **2007**, 55, 669.

(77) Parr, R. G.; Yang, W. *Density-Functional Theory of Atoms and Molecules*; Oxford University Press: New York, **1989**.

(78) Ehrhart, P.; Jung, P.; Schultz, H.; Ullmaier, H. *Atomic Defects in Metal*; Springer-Verlag: Berlin, **1991**; Vol. 25.

(79) Foiles, S. M. *Physical Review B* **1994**, 49, 14930.

(80) Beuerle, T.; Pawellek, R.; Elsasser, C.; Fahnle, M. *Journal of Physics: Condensed Matter* **1991**, 3, 1957.

(81) Frank, W.; Breier, U.; Elsässer, C.; Fähnle, M. *Physical Review B* **1993**, 48, 7676.

(82) Jansen, R. W.; Klein, B. M. *Journal of Physics: Condensed Matter* **1989**, 1, 8359.

(83) Mehl, M. J.; Klein, B. M. *Physica B: Condensed Matter* **1991**, 172, 211.

(84) Vita, A. D.; Gillan, M. J. *Journal of Physics: Condensed Matter* **1991**, 3, 6225.

(85) Benedek, R.; Yang, L. H.; Woodward, C.; Min, B. I. *Physical Review B* **1992**, 45, 2607.

(86) Chakraborty, B.; Siegel, R. W.; Pickett, W. E. *Physical Review B* **1981**, 24, 5445.

(87) Denteneer, P. J. H.; Soler, J. M. *Journal of Physics: Condensed Matter* **1991**, 3, 8777.

(88) Gillan, M. J. *Journal of Physics: Condensed Matter* **1989**, 1, 689.

(89) Pawellek, R.; Fahnle, M.; Elsasser, C.; Ho, K. M.; Chan, C. T. *Journal of Physics: Condensed Matter* **1991**, 3, 2451.

(90) Chetty, N.; Weinert, M.; Rahman, T. S.; Davenport, J. W. *Physical Review B* **1995**, 52, 6313.

(91) Braun, P.; Fähnle, M.; van Schilfgaarde, M.; Jepsen, O. *Physical Review B* **1991**, 44, 845.

(92) Dederichs, P. H.; Hoshino, T.; Drittler, B.; Abraham, K.; Zeller, R. *Physica B: Condensed Matter* **1991**, 172, 203.

(93) Drittler, B.; Weinert, M.; Zeller, R.; Dederichs, P. H. *Solid State Communications* **1991**, 79, 31.

(94) Polatoglou, H. M.; Methfessel, M.; Scheffler, M. *Physical Review B* **1993**, 48, 1877.

(95) Korhonen, T.; Puska, M. J.; Nieminen, R. M. *Physical Review B* **1995**, 51, 9526.

(96) Dederichs, P. H.; Drittler, B.; Zeller, R.; Butler, W. H. e. a. *Materials Research Society* **1992**, 185.

(97) Schaefer, H. E. *Physica Status Solidi a-Applied Research* **1987**, 102, 47.

(98) Siegel, R. W. *Proceedings of the 6th International Conference on Positron Annihilation*, North-Holland: Amsterdam, The Netherlands, **1982**.

(99) Balluffi, R. W. *Journal of Nuclear Materials* **1978**, 69-70, 240.

(100) Chadwick, G. A.; Smith, D. A. *Grain Boundary Structure and Properties;* Academic Press: New York, **1976**.

(101) Ropp, R. C. *Solid State Chemistry*, 4th ed., Elsevier: Amsterdam, The Netherlands, **2003**.

(102) Hull, D.; Bacon, D. J. *Introduction to Dislocations*, 4th ed.; Elsevier: Oxford, MA, **2001**.

(103) Gear, C. W. *Numerical Initial Value Problems in Ordinary Differential Equations*; Prentice-Hall: Englewood Cliffs, NJ, **1971**.

(104) Rapaport, D. *The Art of MD Simulations;* Cambridge University Press: Cambridge, UK, **1991**.

(105) Ray, J. R.; Rahman, A. *The Journal of Chemical Physics* **1984**, 80, 4423.

(106) Ray, J. R.; Rahman, A. *Journal of Chemical Physics* **1985**, 82, 4243.

(107) Tallon, J. L. *Physical Review B* **1988**, 38, 9069.

(108) Accelrys, I. *Cerius2 Modeling Environment Release 4.8;* Accelrys Software Inc.: San Diego, **2005**.

(109) Cagin, T. *General Molecular Dynamics Program for Materials* Pasadena, CA, **1997**.

(110) Ogawa, H., *Materials Transactions* **2003**, *47*, 2706.

(111) Frenkel, D.; Smit, B. *Understanding Molecular Simulation from Alogrithms to Applications*; Academic Press: Orlando, FL, **1996**.

(112) Sutton, A. P.; Chen, J. *Philosophical Magazine Letters* **1990**, 61, 139.

(113) Cagin, T.; Kimura, Y.; Qi, Y.; Li, H.; Ikeda, H.; Johnson, W. L.; Goddard, W. A. *MRS Symp. Ser.* **1999**, 554, 43.

(114) Kart, S. O.; Tomak, M.; Uludogan, M.; Cagin, T. *Materials Science and Engineering a-Structural Materials Properties Microstructure and Processing* **2006**, 435, 736.

(115) Kart, S. O.; Tomak, M.; Uludogan, M.; Cagin, T. *Journal of Non-Crystalline Solids* **2004**, 337, 101.

(116) Kart, S. O.; Tomak, M.; Cagin, T. *Physica B: Condensed Matter* **2005**, 355, 382.

(117) Qi, Y.; Cagin, T.; Kimura, Y.; Goddard, W. A. *Physical Review B* **1999**, 59, 3527.

(118) Strachan, A.; Cagin, T.; Goddard, W. A. *Physical Review B* **2001**, 6305.

(119) Qi, Y.; Cagin, T.; Kimura, Y.; Goddard, W. A. *Journal of Computer-Aided Materials Design* **2002**, 8, 233.

(120) Qi, Y.; Cagin, T.; Johnson, W. L.; Goddard, W. A. *Journal of Chemical Physics* **2001**, 115, 385.

(121) Lee, H. J.; Cagin, T.; Johnson, W. L.; Goddard, W. A. *Journal of Chemical Physics* **2003**, 119, 9858.

(122) Ikeda, H.; Qi, Y.; Cagin, T.; Samwer, K.; Johnson, W. L.; Goddard, W. A. *Physical Review Letters* **1999**, 82, 2900.

(123) Cagin, T.; Dereli, G.; Uludogan, M.; Tomak, M. *Physical Review B* **1999**, 59, 3468.

(124) Kart, H. H.; Tomak, M.; Cagin, T. *Modelling and Simulation in Materials Science and Engineering* **2005**, 13, 657.

(125) Kokalj, A. *Journal of Molecular Graphics and Modelling* **1999**, 17, 176.

(126) Kokalj, A. *Computational Materials Science* **2003**, 28, 155.

(127) Kokalj, A.; Causa, M. Scientific Visualization in Computational Quantum Chemistry; Proceedings of High *Performance Graphics Systems and Applications European Workshop*, Bologna, Italy, **2000**.

(128) Panagiotopoulos, A. Z. *Molecular Physics* **1987**, 813.

(129) Panagiotopoulos, A. Z. *Molecular Physics* **1987**.

(130) Panagiotopoulos, A. Z.; Quirke, N.; Stapleton, M. R.; Tildesley, D. J. *Molecular Physics* **1988**, 527.

(131) Smit, B.; Smedt, P. d.; Frenkel, D. *Molecular Physics* **1989**, 931.

(132) Agrawal, R.; Kofke, D. A. *Physical Review Letters* **1995**, 122.

(133) Kofke, D. A. *Molecular Physics* **1993**, 1331.

(134) Kofke, D. A. *Journal of Chemical Physics* **1993**, 4149.

(135) kofke, D. A.; Cummings, P. T. *Molecular Physics* **1997**, 973.

(136) Han, X. J.; Chen, M.; Guo, Z. Y. *Journal of Physics-Condensed Matter* **2004,** 16, 705.

(137) Hehenkamp, T.; Berger, W.; Kluin, J. E.; Lüdecke, C.; Wolff, J. *Physical Review B* **1992**, 45, 1998.

(138) Klemradt, U.; Drittler, B.; Hoshino, T.; Zeller, R.; Dederichs, P. H.; Stefanou, N. *Physical Review B* **1991**, 43, 9487.

(139) Gavini, V.; Bhattacharya, K.; Ortiz, M. *Journal of the Mechanics and Physics of Solids* **2007**, 55, 697.

VITA

Name: Sandeep Kumar Kamani

Address: Arihant Apartments, Flat#402
Pandurangapuram, Beach Road
Visakhapatnam, Andhra Pradesh
India-530 003

Email Address: sandeep.kamani@tamu.edu

Education M.S. in Chemical Engineering at Texas A&M University, 2008
B.Tech. in Chemical Engineering at Andhra University, 2006